**Kaunas University of Technology**

Faculty of
Mathematics and
Natural Sciences

**Al-Farabi Kazakh
National University**

Faculty of Physics and Technology

# Development of the design of an experimental device with a fast neutron spectrum for radiation staining of semiprecious stones

Master's Final Degree Project

**Zhandos Ualzhanov**

Project author

**Assoc. prof. Živilė Rutkūnienė**

Supervisor

**Almaty, 2023**

**Kaunas University of Technology**

Faculty of
Mathematics and
Natural Sciences

**Al-Farabi Kazakh
National University**

Faculty of Physics and Technology

# Development of the design of an experimental device with a fast neutron spectrum for radiation staining of semiprecious stones

Master's Final Degree Project

6211CX015 Applied Physics (M2096T51)

**Zhandos Ualzhanov**

Project author (signature)
(date)

**Assoc. prof. Živilė Rutkūnienė**

Supervisor (signature)
(date)

**Assoc. prof. Vytautas Stankus**

Reviewer (signature)
(date)

**Almaty, 2023**

**Kaunas University of Technology**

Faculty of
Mathematics and
Natural Sciences

**Al-Farabi Kazakh
National University**

Faculty of Physics and Technology

**Zhandos Ualzhanov**

# Development of the design of an experimental device with a fast neutron spectrum for radiation staining of semiprecious stones

Declaration of Academic Integrity

I confirm that the final project under the Author's name and surname on the topic "Development of the design of an experimental device with a fast neutron spectrum for radiation staining of semiprecious stones" is the result of my own independent work; all the provided data and research resultsare correct and have been obtained in an honest manner. None of the parts of this thesis have been plagiarised from any printed, Internet-based or otherwise recorded sources. All direct and indirect quotations from external resources are indicated in the list of references. No monetary funds (unlessrequired by Law) have been paid to anyone for any contribution to this project.

I hereby fully understand that the discovery of any manifestations/cases/facts of dishonesty inevitably results in personally incurring a penalty according to the procedure(s) effective at Kaunas University of Technology.

_____ _____

(name and surname, hand-written) (signature)

**Almaty, 2023**

Ualzhanov, Zhandos. Development of the design of an experimental device with a fast neutron spectrum for radiation staining of semiprecious stones. Master's Final DegreeProject / Assoc. prof. Živilė Rutkūnienė; Faculty of Mathematics and Natural Sciences, Kaunas University of Technology; Faculty of Physics and Technology,Al-Farabi Kazakh
National University.

Study field and area (study field group): Physical Sciences, Physics.

Keywords: neutron spectrum, minerals, irradiation device, semiprecious stones, reactor, carbide filter, topaz.

Almaty, 2023. 50 pages.

## Summary

This study justifies irradiation capsule design calculations used for efficient coloring of topaz in a WWR-K reactor. Various radiation screens used for removing thermal and epithermal neutrons and their influence on the activation of the main impurities in topaz are considered. It is shown that the use of a sandwich screen composed of boron carbide and tantalum decreases the fraction of thermal neutrons by 24% and increases the fraction of fast neutrons by 15%. These are the optimal neutron conditions for topaz irradiation in a WWR-K reactor. Thermal analysis has been performed by means Comsol code and two approaches were taken: conservative and realistic. A thermo-physical analysis with a conservative approach showed that for boron carbide and tantalum screen the temperatures under forced and natural convection modes were 134 ˚C and 274 ˚C, respectively. The temperature of the case body was 75 ˚C with forced cooling and 238 ˚C without cooling. In case of realistic approach, the topaz temperature does not exceed 65 ˚C if regular cooling of the irradiation capsule is ensured. Calculation results showed the importance of the ensure circulation between topaz during irradiation, which makes it possible to reduce the temperature of topaz by almost half.

Ualzhanov, Zhandos. Eksperimentinio greitojo neutronų spektro prietaiso, skirto pusbrangių akmenų radiaciniam dažymui, konstrukcijos sukūrimas. Magistro baigiamojo laipsnio projektas / Doc. prof. Živilė Rutkūnienė; Kauno technologijos universiteto, Matematikos ir gamtos mokslų fakultetas; Al-Farabi Kazachstanas Nacionalinis universitetas, Fizikos ir technologijų fakultetas.

Studijų kryptis ir sritis (studijų krypčių grupė): Fiziniai mokslai, Fizika.

Reikšminiai žodžiai: neutronų spektras, mineralai, švitinimo įtaisas, pusbrangiai akmenys, reaktorius, karbido filtras, topazas.

Almaty, 2023. 50 p.

## Santrauka

Šis tyrimas pateisina švitinimo kapsulės konstrukcijos skaičiavimus, naudojamus efektyviam topazo dažymui WWR-K reaktoriuje. Nagrinėjami įvairūs radiacijos ekranai, naudojami šiluminiams ir epiterminiams neutronams šalinti ir jų įtaka pagrindinių topazo priemaišų aktyvavimui. Parodyta, kad naudojant sumuštinį, sudarytą iš boro karbido ir tantalo, šiluminių neutronų dalis sumažėja 24%, o greitųjų neutronų dalis padidėja 15%. Tai yra optimalios neutronų sąlygos topazu švitinti WWR-K reaktoriuje. Terminė analizė buvo atlikta naudojant Comsol kodą ir buvo taikomi du metodai: konservatyvus ir realistinis. Termofizinė analizė naudojant konservatyvų metodą parodė, kad boro karbido ir tantalo ekrano temperatūra priverstinės ir natūralios konvekcijos režimais buvo atitinkamai 134 ˚C ir 274 ˚C. Korpuso temperatūra buvo 75 ˚C su priverstiniu aušinimu ir 238 ˚C be aušinimo. Esant realistiniam požiūriui, topazo temperatūra neviršija 65 ˚C, jei užtikrinamas reguliarus švitinimo kapsulės aušinimas. Skaičiavimo rezultatai parodė, kaip svarbu užtikrinti cirkuliaciją tarp topazo švitinimo metu, todėl topazo temperatūrą galima sumažinti beveik perpus.

## Table of Contents

## List of Figures

## List of Tables

## INTRODUCTION

As you know, today the deposits of colored semi-precious stones, which were colored naturally, are almost depleted, and the demand for them is growing every day. Therefore, there is a question of replenishing this stock. Therefore, at present, radiation technologies for their staining are used for this. The most common semi-precious stone that is involved in radiation staining is topaz. For this purpose, neutron irradiation is used, which gives topaz colors of various shades of blue, and thereby increases the jewelry value of these stones several times. In the process of irradiation with fast neutrons, various structural defects are formed in the crystal lattice of topaz, which change its optical properties, thereby changing color.

Research nuclear reactors are used as a tool for radiation staining, which have great potential for radiation treatment of topaz crystals. However, this technology is far from perfect and requires a lot of research and work. In this regard, there is a question that in order to create and continue the normal operation of the installation, a corresponding series of studies is needed.

The implementation of such technology is also carried out in Kazakhstan, in a light-water reactor like WWR-K (Almaty, Kazakhstan), where the energy spectrum of neutrons is thermal.

The object of the study is semiprecious stones.

The subject of the study is the formation of optimal conditions for topaz irradiation in the WWR-K reactor.

Purpose of the work: Development of the design of an experimental device for neutron staining of semiprecious stones based on the VVR-K research reactor.

Results of research: Five variants of irradiation device designs have been developed. Neutron-physical and thermophysical calculations for the developed designs of irradiation devices were carried out..

The main objective of this study is to take into account the main physical quantities that characterize the dependence of the thermal conductivity of the system on the shape and size of the particles, as well as the change in thermal conductivity with increasing temperature during irradiation [1-7]. It is necessary to create a model of the irradiation irradiation pencil case (device) with samples and determine the optimal composition. It is also known that when semiprecious stones are irradiated with neutrons, volumetric energy release occurs. In addition, it is known that at sufficiently high temperatures, annealing of defects in crystals is observed, as well as their cracking, which negates the results of irradiation of the stone. Thus, the next step is to determine the permissible radius of the irradiation pencil case, at which compliance with the permissible temperature regime during irradiation will be observed.

The last stage of the study will be the determination of induced activity in the samples after irradiation. In this case, it is necessary to determine which impurity elements are present in the minerals, then simulate their irradiation in the reactor and determine the retention time of the stones after irradiation before they are used by consumers.

Thus, the purpose of this work is to determine and optimize the operating conditions of the vertical experimental channel of the WWR-K reactor for neutron irradiation of semiprecious stones with a fast neutron spectrum.

# 1 DEFINITION OF THE METHODOLOGICAL APPROACH TO THE STUDY

The WWR-K reactor represents a versatile tank-style research reactor incorporating a light-water moderator and coolant system, accompanied by a beryllium reflector for enhanced functionality. One of the main features of the reactor is a large number of irradiation channels. Currently, the WWR-K reactor has ten vertical channels in the core - three in the center and seven in the periphery; five radial horizontal channels; four horizontal channels that emerge from the niche of experimental devices; as well as one through horizontal tangent channel; Twenty vertical experimental channels in a water reflector. The reactor is a powerful source of neutron and gamma radiation and is designed for scientific research in the field of nuclear physics, solid state physics, radiobiology, solving applied problems in the field of ecology and medicine. The reactor was commissioned in 1967 with a thermal capacity of 6 MW [2].

The reactor core is collected from fuel assemblies, while the number of fuel assemblies and the core configuration, as well as the composition of the reflector, can be changed. The reactor has special experimental devices called experimental channels. This is a complex of equipment and devices of the reactor, combined into one system, designed to conduct experimental research at the reactor.The experimental channels of a research nuclear reactor are a significant tool for radiation processing of materials. At present, there is an accumulation of experience in the successful application of these channels in various technologies for the modification of solids. The use of experimental channels covers such areas as the production of radiopharmaceuticals for the diagnosis and treatment of medical conditions, neutron activation analysis of samples, and others. In addition, irradiation of other materials is possible in the experimental channels, with special attention paid to the group of semiprecious stones.

Semi-precious stones are minerals used in jewelry but are much more common in nature than gemstones. Such minerals include amethyst, aquamarine, chrysolite, quartz, agate, etc. Topaz occupies a special place among these minerals as one of the most popular semiprecious stones. Due to the fact that the deposits of natural colored topaz are almost depleted, and the demand for these semiprecious stones is growing, there is a need to expand the technology for modifying the optical properties of colorless natural minerals using ionizing radiation. Topaz is a mineral from the group of aluminosilicates, having the chemical formula $Al_2(F,OH)_2SiO_4$. All colors inherent in topaz, except purple, are radiant in nature, while the purple color is due to $^{+3}Cr$ ions, isomorphically replacing $^{+3}Al$ in the structure of the mineral. If topaz does not contain impurities and defects, they should be colorless. In nature, topaz is usually yellow or yellow-brown, pale blue or colorless. When heated, yellow topaz often turns orange-pink [8,9].

However, natural pink topaz is extremely rare; this color is usually obtained by heating a certain yellow to reddish-brown Brazilian material that contains the chromium needed to produce the pink color. In general, the scheme of color change under the influence of radiation exposure and heating is shown in Figure 1.

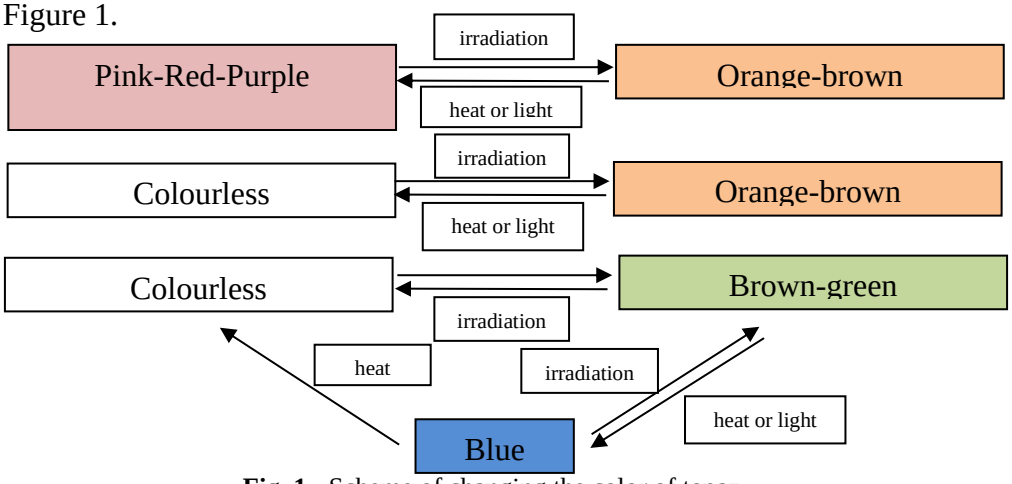


**Fig. 1 -** Scheme of changing the color of topaz

As can be seen from the figure, irradiation is used to give topazes various shades of blue. Several types of irradiations can be used to change the color of topaz: gamma rays, neutrons, and high-energy charged particles such as electrons, protons, and the like [10].
Neutrons in a nuclear reactor can have different energies, as well as be accompanied by gamma rays and other particles. Therefore, both brown and blue colors can be obtained during irradiation in topaz, and heating is used to remove the brown color if blue is required. Figure 2 shows photographs of topaz before irradiation, after irradiation in the reactor with a stream of fast neutrons having shades of brown and blue, as well as after their subsequent heating. Topaz after heating and control of induced radioactivity can be used by the consumer.

Colourless, before irradiation | Blue-brown after irradiation | Swiss blue, after heating

**Fig. 2 –** Effects of radiation and heating on topaz

At present, blue topaz on the market is classified according to the shade of blue as sky blue, Swiss blue and London blue, as shown in Figure 3.

Blue Sky | Swiss Blue | London Blue

**Fig. 3 –** Shades of blue topaz

Thus, in the process of irradiation with fast neutrons, structural disturbances are formed in the topaz crystal that change its optical properties. The optical properties of irradiated topazes, including their optical absorption, are virtually indistinguishable from natural-colored topazes. In the process of neutron irradiation of the crystal structure of topaz, a variety of defects are formed, including simple and complex defective complexes. These complexes of defects are sources of coloring electronic and hole centers.
Obviously, in the development of technology for modifying the optical properties of topaz, it is important to achieve maximum irradiation efficiency, minimum specific activity of minerals and acceptable irradiation temperature in order to avoid damage and turbidity of crystals, as well as annealing of radiation defects.

However, the fulfillment of one of these conditions may have a negative impact on the others. For example, increasing productivity by increasing the volume of irradiation pencil cases can increase the temperature inside the irradiation pencil case and the activity of minerals.

Lowering the temperature by cooling the irradiation pencil case with water can lead to a loss of fast neutron flux density and an increase in mineral activity due to the generation of additional thermal and resonance neutrons. It follows that there are three key factors that need to be considered when designing an irradiation device: performance, irradiation temperature, and radioactivity of topaz after irradiation.

Thus, it is necessary to analyze the neutron-physical conditions and their applicability to the irradiation of semiprecious stones; calculate the temperature regime during irradiation and draw a conclusion about the maximum performance of the channel; In addition, it is necessary to calculate the induced activity in the stones after irradiation and estimate the exposure time of the stones before they are used by consumers. After that, the task is to optimize working conditions, including reducing the unevenness of the impact, as well as increasing labor productivity with a decrease in induced activity.

In this paper, calculations were carried out using Monte Carlo N-Particle Transport Code (MCNP) software. The Monte Carlo Universal N-Particle Transport Code (MCNP) project is aimed at the development and practical use of a computer program for numerical simulation of the transfer of various types of radiation (neutrons, gamma rays, electrons) in three-dimensional systems using the Monte Carlo method. The Monte Carlo method is a numerical method for solving mathematical problems based on the modeling of random variables.

The main advantages of the Monte Carlo method are its ability to simulate the interaction of radiation with matter using information from computational nuclear data files, as well as its flexibility in describing the geometry of systems. In many cases, the Monte Carlo method, together with the calculated nuclear data, can successfully replace the experiment. This class of programs is increasingly used to analyze the radiation and nuclear safety of existing installations and in the design of new nuclear power systems for various purposes.

The MCNP program code is widely used worldwide for neutron-physical calculations of nuclear research reactors, although it can be used for most thermal reactors.

The choice of this software is due to the ability to accurately analyze the processes occurring in the reactor and the absence of the requirement for the user to have extensive knowledge of all user options of the MCNP package. A computational model of the WWR-K reactor core was created using the MCNP package. The approach laid down in the program makes it possible to describe in detail the geometric characteristics and take into account the heterogeneity of the reactor core design.

Thus, on the basis of the existing model of the WWR-K reactor in the MCNP code, it is first necessary to simulate a facility for irradiating semiprecious stones. Before simulating such an irradiation system for the treatment of topaz, it is necessary to consider the physical laws of porous systems, which are the filling of a irradiation pencil case with irradiated stones. It is also necessary to analyze the structural composition of topaz, as well as the effect of the presence of a gas component between the samples on heat transfer during irradiation.

## 2. REVIEW OF EXISTING MODELS OF DEVICES FOR RADIATION COLORING OF SEMIPRECIOUS STONES

The first step of the study is to consider the laws and general physical principles applied to the modeling and calculation of so-called porous physical systems consisting of solid particles in mass, examples of which are irradiated stones filled in an irradiation pencil case. On the basis of these physical principles, subsequent calculations are made in the study.

### 2.1 Device for irradiation of minerals

At the moment, an irradiation device is known, which was used as an invention "Device for irradiating minerals" (Figure 4) [11]. The construction of this innovative facility was established utilizing a conventional 6 MW IRT-T reactor (Tomsk), originating from Tomsk, as its foundation.

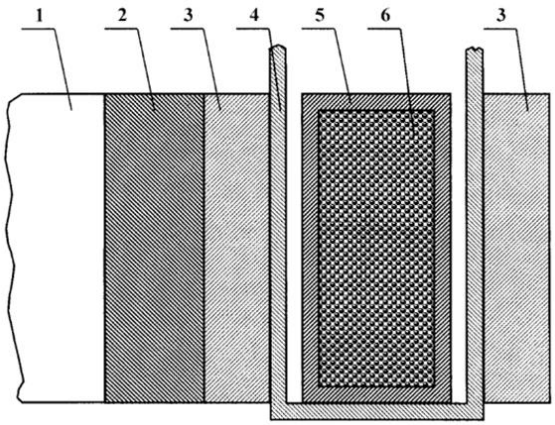


**Fig.4 -** Device for irradiation of minerals

This device includes a nuclear reactor core, a gamma ray absorber, which is a 5 cm thick lead shield capable of providing 12-fold attenuation of gamma quanta, as well as an additional thermal neutron filter with a resonance neutron absorber, consisting of boron carbide with a wall thickness of 1 cm. are also present in the device. The minerals (see Figure 2) are located inside the irradiation pencil case. An additional thermal neutron filter with a resonant neutron absorber is located in the irradiation zone of the irradiation pencil case and surrounds it during irradiation. A thermocouple was used to continuously measure the temperature of the irradiation pencil case during irradiation. The total weight of the irradiated topaz was approximately 1600 g, while the temperature inside the topaz did not exceed 82°C. As a result of irradiation, fast neutron fluence reached a value of $1.1 \cdot 10^{17}$ neutrons/cm$^2$. The minerals received a blue color and have not changed. The technical achievement of the present invention is the possibility of irradiating large volumes of samples at a temperature not exceeding 200°C, which contributes to improving the efficiency of the mineral modification process. The proposed device has a significant advantage, consisting in a significant reduction in the specific energy release in the irradiation pencil case containing samples and filters. This is achieved by using additional absorbers to attenuate gamma rays and resonant neutrons. As a result, it is possible to increase the volume of the irradiation pencil case to accommodate more topazes. Moreover, reducing the fluence of resonant neutrons in the irradiation pencil case automatically reduces the level of induced activity of the irradiated topazes.

### 2.2. The method of irradiation of minerals and the device for its implementation

To achieve irradiation of minerals, a well-known method was used, based on the use of a container wrapped in cadmium foil [12].

Irradiated minerals were placed inside this irradiation pencil case, which were filled with a substance or composition of substances that have the ability to absorb thermal and resonance neutrons, such as

boron-indium, cadmium-tantalum or cadmium-indium. An important aspect was the correct determination of the ratio of these substances in the composition and the achievement of the required filling density of the irradiation pencil case so that certain conditions were met at the time of irradiation, such as $\frac{\varphi_{б.н.}}{\varphi_{т.н.}} \geq 10$, where

$\varphi_{б.н.}$ - fast neutron flux with energies above 1 MeV;

$\varphi_{т.н.}$ - thermal neutron flux.

The above device, which implements the described method, is a irradiation pencil case wrapped in cadmium foil. Irradiated minerals are placed inside this irradiation pencil case, and the space between them is filled with a substance or composition of substances that have the ability to absorb thermal and resonant neutrons.

This method and device make it possible to reduce the undesirable occurrence of induced activity in minerals caused by thermal and resonant neutrons, which are formed as a result of deceleration of fast neutrons in the working volume of the irradiation device.

However, this method and device has the following disadvantages:

1. The useful volume for irradiation of minerals has been reduced.
2. Uneven suppression of activation in the radial direction inside the irradiation device.
3. Long cycle of mineral processing, including preparation, loading, irradiation, aging, discharge and separation of minerals from absorber components.

This invention offers a solution to these problems, which helps to reduce the production of minerals with increased jewelry value.

As an absorbent substance for filtering thermal and resonance neutrons, a composition of boron carbide with aluminum powder is widely used, providing a minimum density of boron carbide at the level of 1.3 g/cm$^3$.

The device for irradiating minerals in the neutron flux of the reactor is designed with a sealed filter unit, in which an axial hole with a cadmium screen is placed, as well as with a pencil case, which is the shape of a cylinder or prism, open at the bottom for partial filling with coolant. Inside the working volume of the pencil case, minerals are mixed with substances that has the ability to absorb thermal and resonance neutrons, and the layers are separated by an aluminum layer.

Each layer of minerals and a substance or composition of substances containing elements capable of absorbing thermal and resonance neutrons can be enclosed in an aluminum shell taking the form of a briquette or glass. To ensure thermomechanical contact, shells with minerals and substances or compositions of substances containing elements that absorb thermal and resonance neutrons can be additionally fixed in the upper part of the pencil case by means of a clamp.

The placement of minerals in layers between layers of a substance or composition of substances containing elements capable of absorbing thermal and resonant neutrons, using an aluminum layer for separation of layers, as well as the placement of a filter unit of a substance or composition of substances containing elements that absorb thermal and resonance neutrons, with a cadmium shield around the layers, provide effective capture of thermal and resonant neutrons to reduce the effect of thermal isolation of fast neutrons on minerals, in order to reduce their activity.

To ensure optimal conditions for irradiation of minerals, including the fulfillment of inequalities $\frac{\varphi_{б.н.}}{\varphi_{т.н.}} \geq 10$ and maintaining the temperature below 200 °C, the calculation and experimental selection of the thickness of the layers and the geometric parameters of the filter unit, such as height and shape, are applied. These irradiation parameters contribute to the production of minerals with increased jewelry value. At the same time, when irradiated at temperatures above 200 °C, degradation of mineral properties, such as cracking, discoloration and transparency, is observed.

The ratio between the thermal neutron flux and the fast neutron flux ($\frac{\varphi_{б.н.}}{\varphi_{т.н.}} \geq 10$) during irradiation, it allows you to control the color of minerals without exceeding the permissible level of induced activity. In the case where the ratio $\frac{\varphi_{б.н.}}{\varphi_{т.н.}} \geq 10$, There is a significant increase in induced activity, which requires prolonged exposure of irradiated minerals and, therefore, increases the time of their

processing. The aluminum layer acts as a heat sink from the central part of the layer and maintains the temperature regime on minerals below 200 °C.

The placement of minerals and a substance or composition of substances containing elements that absorb thermal and resonance neutrons in layers with an aluminum interlayer prevents them from mixing, which eliminates the need for separate processing and significantly reduces the processing time of minerals.

The preferred choice of a substance containing elements that absorb thermal and resonance neutrons is naturally enriched boron carbide, as well as oxides of dysprosium, hafnium, gadolinium and other elements.

Alternatively, a composition of naturally enriched boron carbide with aluminum powder can be used, with the possible inclusion of dysprosium, hafnium and/or gadolinium oxides for dispersion purposes [12].

The choice of a composition comprising a composition of boron carbide and aluminum powder as a substance containing elements capable of absorbing thermal and resonant neutrons in a filter unit with a boron carbide minimum density of 1.3 g/cm3 is required to ensures optimal filtration of thermal and resonant neutrons, as well as efficient heat dissipation. In the case where the density of boron carbide is lower than the specified value, reliable capture of thermal and resonant neutrons cannot be guaranteed.

Using a cylindrical or prismatic shape, a pencil case containing minerals and a substance or composition of substances that have the ability to absorb thermal and resonance neutrons, in layers and open at the bottom for partial filling with coolant, eliminates the need to seal the irradiation device. This ensures that the required irradiation conditions are maintained, prevents water from entering the mineral area, simplifies the loading and unloading process, and ensures that this device can be reused.

The presence of a safety valve in the filter unit to remove helium and tritium formed during irradiation ensures effective and safe irradiation of minerals.

Packing each layer of minerals and a substance or composition of substances containing elements capable of absorbing thermal and resonant neutrons in an aluminum shell in the form of a briquette or beaker ensures fast and safe loading and unloading. There is also the possibility of reusing, for example, aluminum cups or briquettes containing boron carbide.

To improve heat dissipation between shells with minerals and a substance or composition of substances that absorb thermal and resonant neutrons, a clamp is used.

In the existing scientific and technical literature, no new significant characteristics inherent in the claimed invention have been found. Therefore, the proposed solution is not obvious on the basis of existing achievements. The set of these characteristics has new properties, which allows us to conclude that this solution meets the criterion of the innovation level.

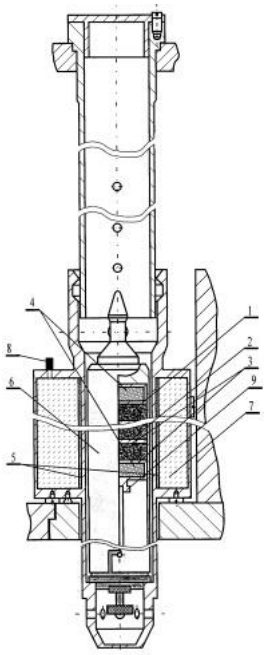

**Fig.5 -** Method of irradiation of minerals and the device for its implementation

Figure 5 is a vertical cross-section of the apparatus designed for the procedure of irradiation of mineral samples, where:

1 - layer of minerals;
2 - a layer of matter that absorbs thermal and resonance neutrons;
3 - aluminum interlayer;
4 - cadmium discs;
5 - cadmium screen;
6 - pencil case;
7 - filter Unit;
8 - safety valve;
9 - clamp.

The proposed device for irradiation of minerals includes a sealed filter unit (7), having dimensions of $2,5 *10^{-2} – 4,5 *10^{-2}$ m and consisting of a composition of boron carbide with aluminum powder. This apparatus is designed for the absorption of thermal and resonant neutrons. It contains a central cavity where the cadmium screen (5) is positioned. Additionally, the device includes a cylindrical container (6) measuring approximately 450 mm in height, which is filled with mineral layers (1) of approximately 80-90 mm thickness. To separate these layers, a thin aluminum sheet measuring 0.2 mm in thickness is utilized.

For the procedure of irradiation of minerals, a special apparatus in the form of a cylindrical pencil case (designated as 6) is used, which allows you to sequentially load briquettes of minerals (designated as 1) and briquettes with neutron-absorbing materials, such as boron carbide (designated as 2), wrapped in an aluminum shell. The thickness of briquettes with minerals and neutron-absorbing materials is determined by experimental and computational studies for various types of minerals in order to achieve a given level of suppression of thermal and resonance neutrons. This level is achieved with an induced specific activity of minerals not exceeding 74 Bq/g after irradiation to a certain intensity of fast neutrons (about $1 \cdot 10^{18}$ cm-2), as well as with a subsequent two-week exposure.

The pencil case (designated as 6) has a design with a closed upper end and an open lower end. It is installed in the filter unit (designated as 7), which is located in the water of the reactor reflector. The air cavity inside the pencil case and the volume of air were selected in such a way that the water level

did not reach the column of briquettes, which is held in the upper part of the pencil case by means of a clamp (designated as 9).

The filter unit (designated as 7) is a sealed cavity filled with a composition of boron carbide and aluminum powder. The column of briquettes is surrounded by a cadmium screen (labeled as 5) and upper and lower cadmium discs (labeled as 4).

The transfer of heat from minerals, due to radiative energy release, is carried out radially to the wall of the pencil case using an aluminum layer (designated as 3), which serves as a shell for briquettes (designated as 1) and (designated as 2). After a predetermined irradiation period, the pencil case is removed, and the mineral briquettes are extracted after aging.

Irradiation of minerals in the reactor is carried out by fast neutrons with an energy of at least 0.5 MeV at an integral radiation dose in the range from $0.2 \cdot 10^{12}$ to $2 \cdot 10^{12}$ neuters/cm$^2$ and a temperature not exceeding 200 °C for 40-50 hours, which leads to the achievement of fast neutron fluence from $2.2 \cdot 10^{17}$ to $7.2 \cdot 10^{17}$ neutr/cm$^2$.

The thickness of briquettes with boron carbide, used to suppress thermal and resonant neutrons, was determined as a result of experiments and is predominantly 2-3 mm. Boron carbide in briquettes is carefully packed in aluminum foil with a thickness of mainly 0.2 mm.

Such packaging provides effective heat removal from the central part of the briquettes to the wall of the pencil case, thereby ensuring the convenience and safety of their loading and unloading, as well as the possibility of repeated use.

Through experimental analysis, it has been established that the layers containing minerals exhibit a consistent thickness of approximately 80-90 mm. To enhance thermal management, these layers are carefully enveloped with aluminum foil, typically measuring 0.2 mm in thickness. The aluminum foil serves a critical function in facilitating heat transfer from the central region of the mineral layer to the pencil case wall, effectively preventing the stones from exceeding a temperature threshold of 200 °C.

The geometric dimensions of the filter block were determined using a computational and experimental approach to ensure the ratio $\frac{\varphi_{\text{б.н.}}}{\varphi_{\text{т.н.}}} \geq 10$. These dimensions include predominantly a block height of 450 mm, a thickness of the neutron filter material in the block in the range from 25 to 45 mm and a central hole diameter of 70 mm.

In the course of the experimental work of this model, samples of various types were irradiated.

Option 1. In this embodiment, topaz crystals were used in irradiation, the thickness of which was determined experimentally and was mainly 2-3 mm. Boron carbide in briquettes is packed in aluminum foil with a thickness of 0.2 mm, which ensures effective heat removal from the center of the briquettes to the wall of the pencil case and ensures their fast and safe loading and unloading. With such a configuration, there is the possibility of repeated use. As a result of irradiation, colorless topazes undergo a color change, namely from light blue to dark blue.

Option 2. The second option involves irradiating faceted colorless topaz crystals. The briquette contained a mixture of boron carbide with dispersed hafnium oxide, which served to suppress thermal and resonance neutrons. The thickness of the briquette was also determined experimentally, approximately 2-3 mm. In these briquettes, boron carbide with hafnium oxide is packed in aluminum foil with a thickness of mainly 0.2 mm.

Option 3. The third option also describes the irradiation of faceted products made of colorless topaz crystals. But the briquette in this case contains already dispersed gadolinium oxide and a mixture of boron carbide, the thickness of which is about 2-3 mm. In these briquettes, boron carbide with gadolinium oxide is packed in aluminum foil with a thickness of mainly 0.2 mm.

Option 4. In the case of irradiation of rock crystal products in the peripheral channel of the reactor, the fluence of fast neutrons reached approximately $1 * 10^{16}$ cm$^{-2}$. In order to filter thermal and resonant neutrons, a mixture of boron carbide and aluminum powder was used. The result of irradiation was the smoky-gray color of the samples. If the fluence increases, the color of the samples darkens, turning into black, but thereby increases the radioactivity of minerals.

Option 5. Irradiation of weakly colored beryl crystals was carried out in the peripheral channel of the reactor at a fluence of approximately $1*10^{18}$ $cm^{-2}$. The filter was a mixture of boron carbide with dispersed hafnium oxide, which is necessary for the capture of thermal and resonant neutrons. The samples in this case received an intense yellow color. An increase in fluence in this case does not make sense, since the radioactivity of the samples also increases.

Minerals irradiated in the device according to the presented method showed a change in color while maintaining their transparency. The resulting color turned out to be resistant to light (ultraviolet radiation). Irradiated minerals have acquired an increased jewelry value. It is important to note that the production cycle of minerals has been reduced by 1.5-2 times compared to known methods.

But it is important to note that this method and device have certain drawbacks.

1. This is a decrease in the useful volume for irradiation of minerals, providing a small volume of irradiated minerals in the irradiation process.
2. Uneven suppression of activation in the radial direction inside the irradiation device.
3. Long mineral processing cycles, including preparation, loading, irradiation, aging, discharge and separation of minerals from absorber components.

The literature review provided unveils that an indispensable element within irradiation capsules, utilized for proficient radiation staining of topaz in nuclear reactors, is a shield composed of one or more substances. The primary aim of this research is to devise a specialized capsule for irradiating topaz with radiation in a WWR-K reactor, employing Monte Carlo techniques and the finite element method. This study delves into the physical attributes of the capsule, while considering the impact of various capsule screens and the interplay between neutron-physical and thermal screen effects.

## 3 EXPERIMENTAL SETUP AND MEASUREMENT TECHNIQUE

### 3.1 Experimental setup and measurement technique

The newly developed irradiation device has been specifically designed for use in the WWR-K reactor and is compatible with any cell within its core. The calculations were conducted with a focus on an irradiation position strategically positioned at the center of the active zone within the WWR-K reactor. In essence, the WWR-K reactor is a tank-style research reactor equipped with a light water moderator and coolant system, complemented by a beryllium neutron reflector (as depicted in Figure 6). The neutron energy spectrum specific to the WWR-K reactor has been provided. To maintain standard cooling, the core operates with a coolant flow rate of approximately 600 m3/h. Notably, the WWR-K reactor is a versatile facility with extensive applications [13–21]. Figure 6 illustrates that the undisturbed core comprises 48% thermal neutrons and 25% fast neutrons [22,23]. Accordingly, it is imperative that the neutron energy distribution in an ED be inverted, wherein the fraction of fast neutrons surpasses that of thermal neutrons [2].

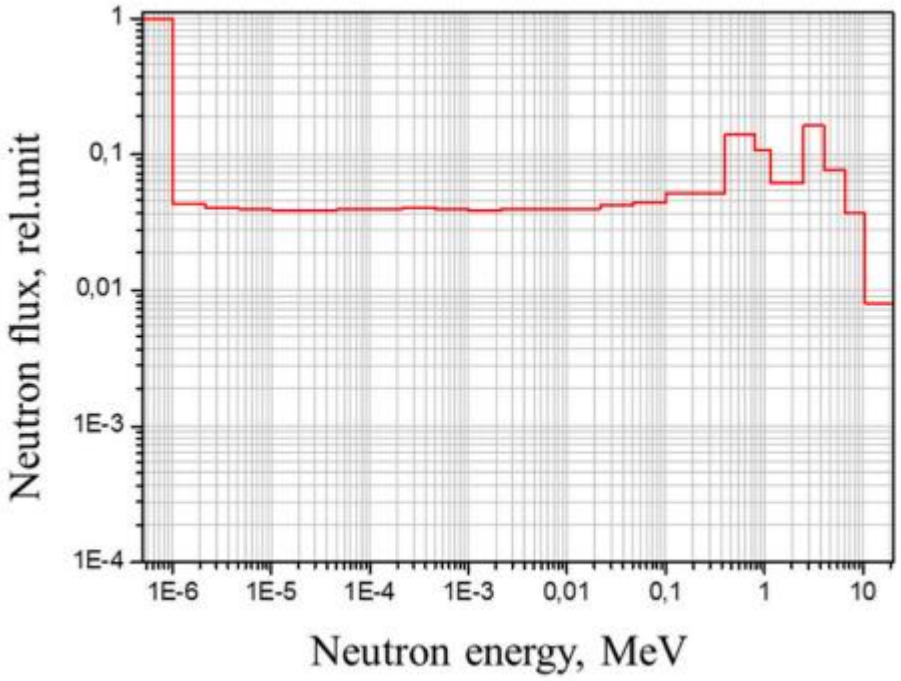


**Fig.6 -** Energy spectrum of neutrons in the considered irradiation position of the WWR-K reactor

### 3.2. Development of the design of the irradiation device

The irradiation device is a pencil case with topaz and various types of radiation shields that modify the density and spectrum of neutrons that irradiate topaz and form a heat source under the action of reactor radiation. The case is immersed in the water irradiation channel of the reactor so that the middle of the height of the case is at the level of center of the reactor core. The water interspace between the wall of the case and the wall of the channel is 1 mm. The wall of the channel is an aluminum pipe with a thickness of 3 mm, the external surface of the pencil case is in contact with the water flowing through the cooling system of the reactor. The temperature of water in channel and the initial temperature of the device is 40 ° C. Schematic view with the dimensions of the pencil case is shown in Figure 7. A single radiation shield has a thickness of 1 mm, a double-layer - 2 mm and covers the inner surface of the vertical wall of the pencil case [2].

Within the configuration depicted in Figure 7, topaz is positioned within a specialized shielding structure intended to alter the neutron flux and spectral characteristics. The chemical composition of topazes employed in the computations is denoted by the formula $Al_2SiO_4(F,OH)_2$. n the analysis,

various substances were evaluated as shielding options, including boron carbide, cadmium, tantalum, as well as their respective combinations. It is important to note that all the materials taken into account possess natural isotopic compositions.
Table 1 provides the atomic densities of all the materials being examined.

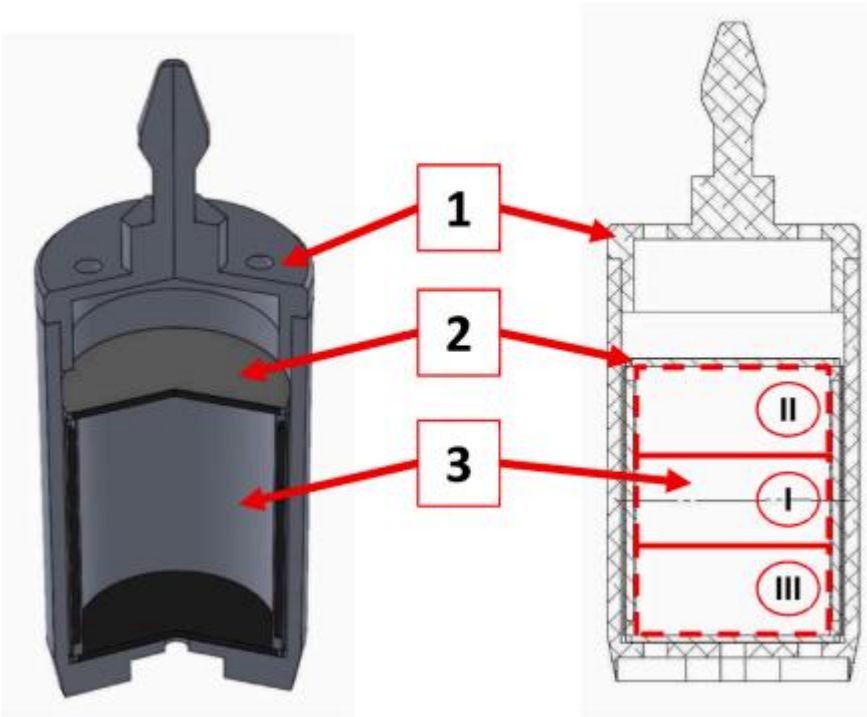


**Fig.7 –** Represented in both volumetric and schematic forms, the irradiation device exhibits distinct components: 1 - an aluminum capsule; 2 - a screen; and 3 - a designated space for housing the topaz material

**Fig.8 –** Appearance of topaz

**Table 1 -** The composition of the materials used in the irradiation device is as follows:

| Element | Atomic density * $10^{-2}$ at/barn*cm |
|---|---|
| ***Regular capsule*** | |
| Al | 5.91 |
| ***Topaz stones $Al_2[SiO_4]$ $(OH, F)_2$*** | |
| H | 1.98 |
| Al | 1.98 |
| Si | 0.99 |
| O | 5.93 |
| F | 1.98 |
| ***boron carbide $B_4C$*** | |
| B | 7.32 |
| C | 1.83 |
| ***Tantalum*** | |
| Ta | 5.54 |
| ***Cadmium*** | |
| Cd | 4.63 |

The energy dissipation of each of the pencil case materials for the five variants of the pencil case (depending on the screen material) is shown in Tables 2-6 below. The energy dissipation indicated in the tables is given for the level of the center of the reactor core (in Figure 8 it is bounded by red dotted lines), the heat dissipation outside this zone is 10% less [2].

**Table 2 –** Energy dissipation of materials, option 1

| Material | Radiative heating, W/g | Density, g/cm$^3$ | Radiative heating, W/cm3 |
|---|---|---|---|
| SAV-1 (pencil case wall) | 2.77 | 2.7 | 7.48 |
| Boron carbide (screen inside the pencil case) | 34.47 | 2.52 | 86.86 |
| Topazes | 2.90 | 3.56 | 10.32 |

**Table 3 –** Energy dissipation of materials, option 2

| Material | Radiative heating, W/g | Density, g/cm$^3$ | Radiative heating, W/cm3 |
|---|---|---|---|
| SAV-1 (pencil case wall) | 2.86 | 2.7 | 7.72 |
| Tantalum (screen inside the pencil case) | 6.02 | 16.654 | 100.25 |
| Topazes | 2.96 | 3.56 | 10.54 |

**Table 4 –** Energy dissipation of materials, option 3

| Material | Radiative heating, W/g | Density, g/cm$^3$ | Radiative heating, W/cm3 |
|---|---|---|---|
| SAV-1 (pencil case wall) | 2.65 | 2.7 | 7.16 |

| | | | |
|---|---|---|---|
| Cadmium (screen inside the pencil case) | 25.99 | 8.65 | 224.8 |
| Topazes | 2.89 | 3.56 | 10.29 |

**Table 5 –** Energy dissipation of materials, option 4

| Material | Radiative heating, W/g | Density, g/cm$^3$ | Radiative heating, W/cm3 |
|---|---|---|---|
| SAV-1 (pencil case wall) | 2.51 | 2.7 | 6.74 / 6.07 |
| Tantalum | 5.31 | 16.654 | 88.43 / 75.99 |
| Boron carbide | 28.95 | 2.52 | 72.95 / 65.66 |
| Topazes | 2.69 | 3.56 | 9.58 / 8.62 |

**Table 6 –** Energy dissipation of materials, option 5

| Material | Radiative heating, W/g | Density, g/cm$^3$ | Radiative heating, W/cm3 |
|---|---|---|---|
| SAV-1 (pencil case wall) | 2.64 | 2.7 | 7.13 / 6.41 |
| Cadmium | 16.00 | 8.65 | 138.4 / 124.5 |
| Boron carbide | 21.11 | 2.52 | 53.2 / 47.88 |
| Topazes | 2.83 | 3.56 | 10.07 / 9.07 |

3.3 Neutron-physical and thermophysical calculations

By employing the Monte Carlo method and utilizing the MCNP6 transport code alongside the ENDF/B-VII.1 program [24,25], neutron-physical calculations were conducted for the irradiation apparatus, considering diverse screen materials such as boron carbide, tantalum, cadmium, boron and tantalum carbide, as well as boron carbide and cadmium. The MCNP6 transport code operates through stochastic simulations, simulating the interactions between neutrons, other particles, and the surrounding matter. This comprehensive program enables the computation of various functions that represent convolutions between the flux of neutron or photon and nuclear physics data. All computations within this study are standardized based on the original particle, which is further normalized to the generation of fission neutrons. Flow analysis was conducted utilizing the F4 count (Cell Flow Track Length Estimate). Furthermore, the neutron energy levels can be accurately determined using the E4 energy meter. The flow outcomes were precisely calibrated at a power level of 6 MW, employing a conversion coefficient of 5.12*1017. When conducting power distribution calculations, the F6 accounting cards N and P were utilized in combination with the "ACT FISSION = ALL" map, which incorporates delayed photons and neutrons for an accurate estimation of the length of the energy release path. Each input file comprised a total of 400 cycles, including 40 inactive cycles and 360 active cycles, with 100,000 stories per cycle. It should be noted that the accuracy of the calculations is directly proportional to the extent to which the Monte Carlo model accurately represents the real-world scenario. The utilization of a comprehensive heterogeneous model yielded highly precise outcomes, particularly in regard to characterizing the core of the WWR-K reactor. This simulation method incorporated the genuine composition of the reactor core, accounting for fuel burnout within fuel assemblies, as well as the effects of beryllium neutron reflector poisoning. Considering the high-density presence of topaz within the capsule volume, they were treated as a homogeneous medium in the calculations. It is noteworthy that the statistical error of the calculations remained below 5%, further affirming their reliability.

The computation was executed employing the versatile COMSOL Multiphysics software [26], specifically designed for simulating intricate physical phenomena. To facilitate the calculation process, an axially symmetrical geometry was employed, featuring a simplified yet physically valid representation of the irradiation setup. This geometry accurately portrayed the structure and

dimensions of the irradiation capsule containing the irradiated topaz samples, along with the radiation screen(s), as well as the surrounding components of the irradiation channel. These components included the water regions situated above and below the capsule, the aluminum alloy wall of the WWR-K channel, and a 1-mm water gap separating the channel wall and the irradiation capsule.

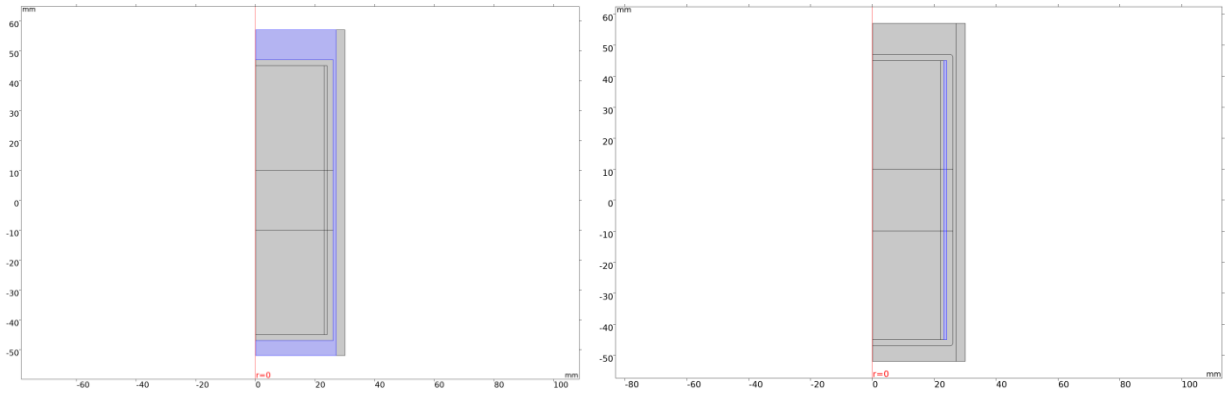

**Fig.9 –** Variants of the calculated geometry: on the left is a single-layer screen (blue shows the water area), on the right - a two-layer screen (cadmium is shown in blue)

Figure 10 shows the calculated geometries for the case of a single-layer and double-layer radiation shield. Two horizontal lines passing through the middle of the pencil case show the areas of geometry (domains) where the heat dissipation will be maximum, corresponding to the values from Tables 2-6.

It is believed that topaz is densely filled in a pencil case and is a homogeneous medium. According to the work of D.B. Hoover [27], the thermal conductivity of topaz is assumed to be 18.67 W/(m*K). To describe the thermophysical properties of the remaining materials, the COMSOL Standard Material Library (for aluminum, tantalum, boron carbide, cobalt) was used. This means that all the parameters necessary for the thermal calculation (thermal conductivity k, heat capacity at constant pressure $C_p$ and density p) and their temperature dependences are taken from a proven source. However, according to the $T_K$, the density of boron carbide was fixed at a value of 2.52 g/cm$^3$.

The computation employed a comprehensive analytical framework encompassing essential heat transfer equations, which accounted for thermal conductivity, convection, and thermal radiation. A nonisothermal water flow model, integrating equations for thermal conductivity in both solid and liquid media with the Navier-Stokes equation, was utilized to describe the laminar or turbulent movement of cooling water flows.

Equations of thermal conductivity and convection:

$$\rho C_p \frac{\partial T}{\partial t} + \rho C_p \boldsymbol{u} \cdot \nabla T + \nabla \cdot \boldsymbol{q} = Q + Q_p + Q_{vd} \quad (1)$$

$$\boldsymbol{q} = -k\nabla T \quad (2)$$

Equations for heat transfer by radiation (surfaces):

$$-\boldsymbol{n} \cdot \boldsymbol{q} = \varepsilon(G - e_b(T)) \quad (3)$$

$$(1 - \varepsilon)G = J - \varepsilon e_b(T) \quad (4)$$

$$G = G_m(J) + G_{amb} + G_{ext} \quad (5)$$

$$G_{amb} = F_{amb} e_b(T_{amb}) \quad (6)$$

$$G_{ext} = G_{extDir} + G_{extDiff} \quad (7)$$

$$e_b(T) = n^2 \sigma T^4 \quad (8)$$

The governing equations for laminar flow encompass the Navier-Stokes equations, which account for the conservation of momentum, as well as the equations of continuity, which ensure the conservation of mass:

$$\rho \frac{\partial \boldsymbol{u}}{\partial t} + \rho(\boldsymbol{u} \cdot \nabla)\boldsymbol{u} = \nabla \cdot \left[ -p\boldsymbol{I} + \mu(\nabla \boldsymbol{u} + (\nabla \boldsymbol{u})^T) - \frac{2}{3}\mu(\nabla \cdot \boldsymbol{u})\boldsymbol{I} \right] + \boldsymbol{F} + \rho \cdot \boldsymbol{g} \quad (9)$$

$$\frac{\partial \rho}{\partial t} + \nabla \cdot (\rho \boldsymbol{u}) = 0 \quad (10)$$

Hereinafter, the following designations are used:

- $p$ - density (kg/m$^3$)
- $C_p$ - specific heat at constant pressure (J/(kg*K))
- $T$ - absolute temperature (K)
- **u** - velocity vector (m/s)
- **q** - heat flux vector (W/m$^2$)
- $Q$ - internal heat sources (W/m$^3$)
- $Q_p$ - heat caused by pressure (W/m$^3$)
- $Q_{vd}$ - heat of internal friction (W/m$^3$)
- $k$ - thermal conductivity (W/(m· K))
- **n** - normal vector outward
- n - the refractive index for a transparent medium (dimensionless)
- ε - surface emissivity (dimensionless)
- μ - dynamic viscosity (Pa*s)
- $G$ - incident flow (W/m$^2$)
- $J$ - radiant flux (W/m2)
- $G_{amb}$ - ambient flow (W/m2)
- $G_{amb,d}$ - ambient flow, underside (W/m2)
- $G_{amb,u}$ - ambient flow, upper side (W/m2)
- $G_d$ - flux incident on the bottom surface (W/m2)
- $G_u$ - flow incident on the upper surface (W/m2)
- $G_{ext}$ - external flow (W/m2)
- $G_m$ - mutual surface radiation (W/m2)
- $F_{amb}$ - appearance factor (dimensionless)
- $T_{amb}$ - ambient temperature (K)
- $\sigma$ - Stefan-Boltzmann constant (W/(m$^2$ * K$^4$))
- $e_b(T)$ - total blackbody radiation power (W/m2)
- $\nabla$ - differentiation operator, NABLA (m$^{-1}$)
- **I** - unit tensor (dimensionless)

According to the task of the research project, it is necessary to calculate the stationary distributions of temperatures and velocities of water movement in the computational region for two cases of water

cooling: 1) - water is forcibly supplied from the upper area above the case at a speed of 0.3 m/s down through the gap of the case channel; 2) There is no forced water supply, the water moves freely between the upper and lower water cavities under the action of convection.

3.4 Description of initial and boundary conditions

Table 7 provides an overview of the primary boundary conditions utilized in the thermophysical computations.

**Table 7 –** The fundamental boundary conditions applied in the thermophysical calculations for the irradiation facility are outlined below.

| Boundary conditions | Count |
|---|---|
| Thermal conductivity of topaz, W/m*K | 18.67 |
| Thermal conductivity of the aluminum layer, W/m*K | 240 |
| Thermal conductivity of boron carbide, W/m*K | с 32.5 (at 300K) до 21.5 (at 600K) |
| Thermal conductivity of cadmium, W/m*K | с 97 (at 300K) до 88 (at 600K) |
| Thermal conductivity of tantalum, W/m*K | с 57.5 (at 300K) до 58.7 (at 600K) |
| Topaz density, g/cm$^3$ | 3.56 |
| Density of boron carbide, g/cm$^3$ | 2.52 |
| Density of cadmium, g/cm$^3$ | 8.65 |
| Density of tantalum, g/cm$^3$ | 16.65 |
| Density of the aluminum layer, g/cm$^3$ | 2.7 |
| Coolant temperature, $^o$C | 40 |
| Coolant flow rate, m/s | 0.3 |
| The direction of movement of the coolant | Down |

The starting conditions consisted of assigning an initial temperature of 40 °C to all materials within the model. The pressure was maintained at the atmospheric level, considering the hydrostatic contribution determined by the height of the water column. Perfect thermal contacts were assumed throughout the system, guaranteeing the absence of any discontinuities during the heating process.

Phase transitions of water and other materials were not considered in the heating process. A conservative approach was taken in the calculations regarding the description of topaz within the screen, omitting the consideration of water circulation among the minerals.

Considering practical constraints and the computational limitations that prevent the inclusion of the entire water volume in the model, boundary conditions were defined for the upper and lower boundaries of the water region (indicated in blue color in Fig. 10). These boundary conditions accounted for convection heat transfer with the bulk of the water in the respective positions, adhering to the specified law:

$$Q_0 = h \cdot (T_{ext} - T) \quad (11)$$

In the equations provided, $Q_0$ represents the specific convective heat flux per unit area. T represents the calculated water temperature near the case, while Text represents the external temperature of the water within the cooling system of the reactor. The convection coefficient for heated water is denoted as h = 0.3 W/(cm$^2$*K).

Figure 10 also illustrates the condition where the outer surface of the channel wall, in contact with the water array of the reactor cooling circuit, maintains a fixed temperature of $T=T_{ext}$. This condition signifies the strong cooling of the channel wall by the external water.

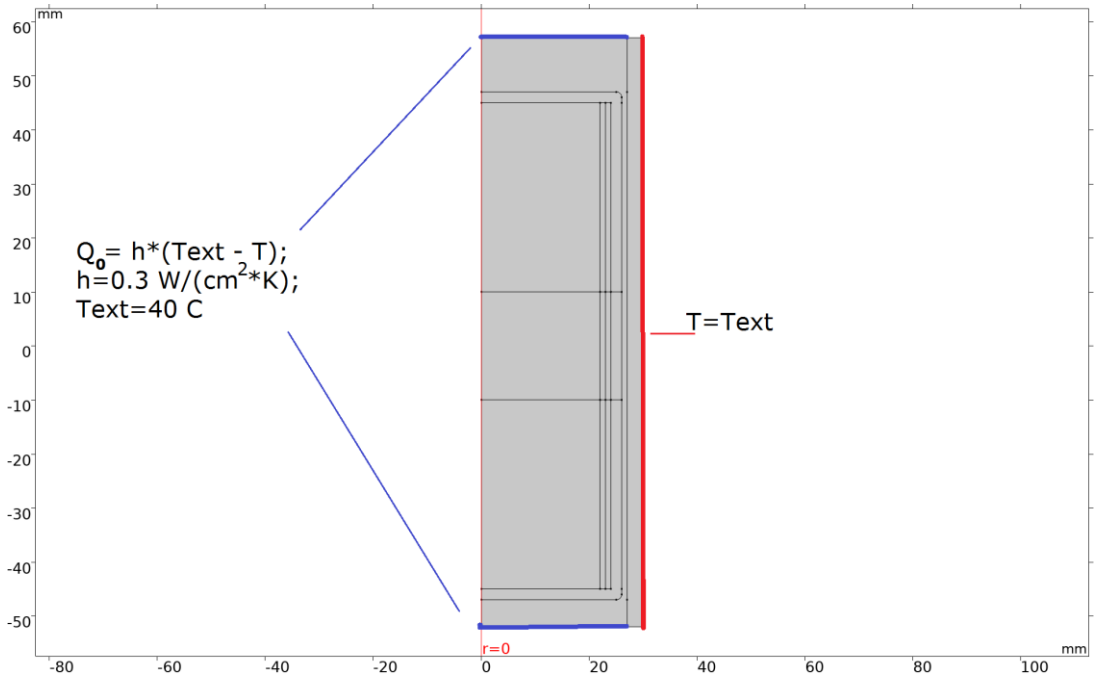


**Fig.10 -** In the analysis, convective heat transfer of water was governed by boundary conditions at the blue boundaries, while the outer surface of the channel had a fixed temperature specified at the red boundary

Next, in the model settings, heat was assigned to materials that generate heat when exposed to radiation, according to Tables 2-6 for five different tasks. An example of the purpose of heat dissipation for task 6 (boron carbide with cobalt) is shown in Figure 11.

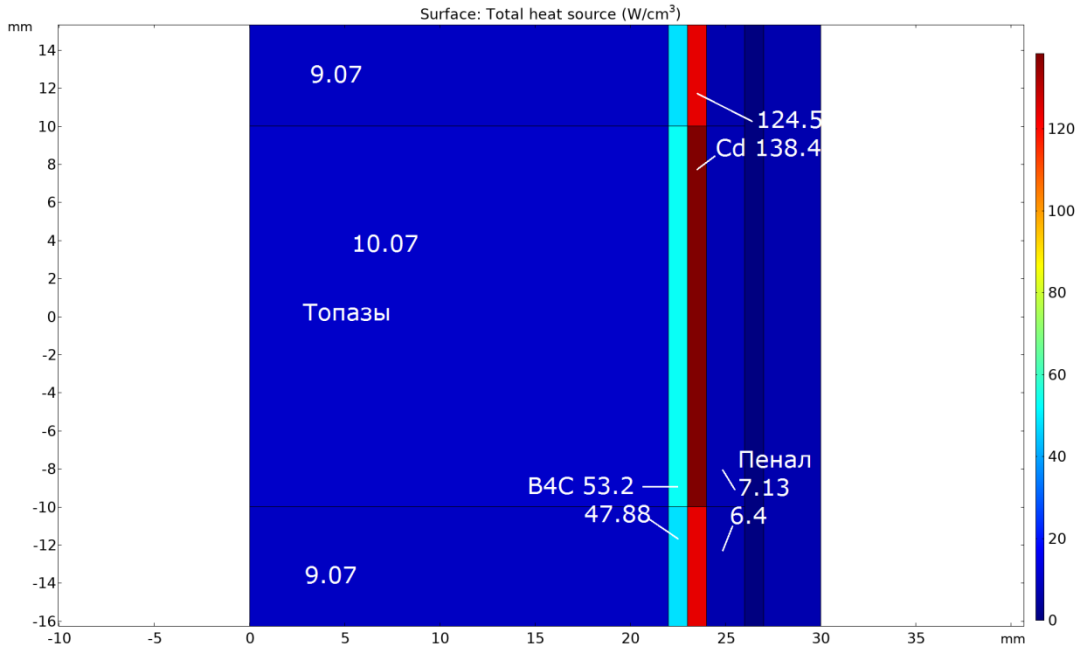


**Fig.11 -** Example of the specific heat dissipation of model materials, taken from task No. 5. Values are given in W/cm$^3$

The model incorporates radiative energy transfer between the pencil case and the channel wall through the water, following Stefan Boltzmann's law. The surfaces' emission properties are characterized by ε=0.3.

In the simulation, water flow is modeled as a weakly compressible liquid to represent laminar flow during forced pumping and free convection. All surfaces in contact with water are assumed to have

friction (No Slip) regardless of flow velocities. The upper boundary of the water, depicted in Figure 3, is designated as the inlet (Inlet), where convection heat exchange occurs with the channel water. The water flow on this boundary is directed downward, perpendicular to the surface, with a velocity of 0.3 m/s for forced cooling and 0.1 mm/s for convection movement. The lower boundary of the water in the model is referred to as the water runoff area (Outlet), where gravity acts as a downward force on the water, creating conditions for convection in the absence of other external forces.
The grid of approximation of the problem by finite elements is shown in Figure 12.

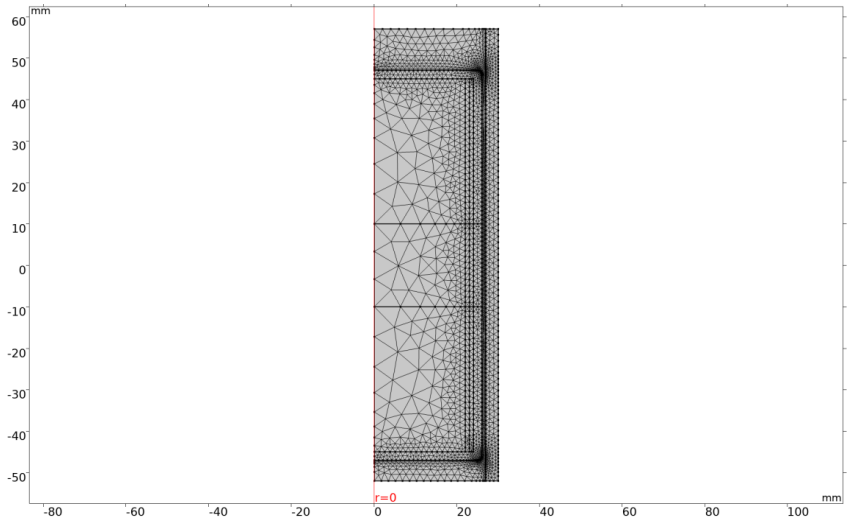


**Fig.12 -** Grid approximation of the modeling area by finite elements

Each of the five separate tasks was also counted separately for the two modes of water movement. As it turned out from practice, the calculation of the stationary temperature field and the distribution of the velocity and direction of water flows during forced cooling of the pencil case was better and faster considered by the stationary PARDISO solver, and the convection mode was better considered in the Time Dependent mode. The calculation of the "convection problem" was performed for a convection process duration of 1000 seconds, which was sufficient to achieve a stationary state (Figure 13).

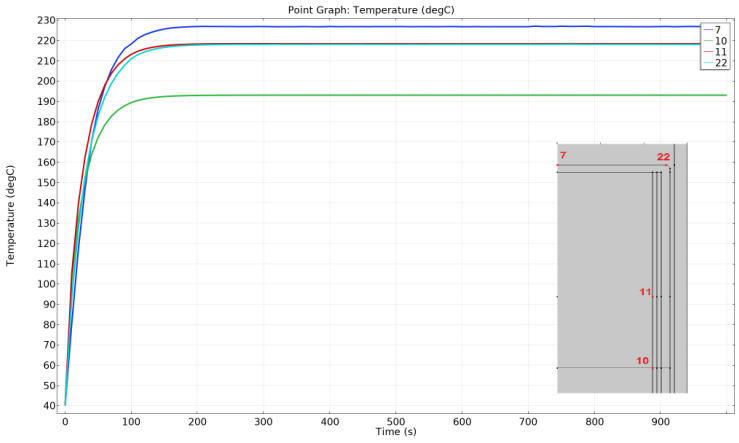


**Fig.13 –** The process of establishing stationary temperatures at four control points in the simulation of the process of establishing convection flows after turning off the water supply (task No. 4). On the tab - the location of control points in the model and their numbers

## 4. GENERAL ANALYSIS OF THE RESULTS

Before selecting the screen material for the irradiation device, a neutron activation analysis was performed to identify the activated impurities in topaz. The topaz samples were irradiated in the WWR-K reactor using a standard irradiation capsule that did not include any screens. To measure the resulting induced activity of the minerals, a gamma spectrometer with a Canberra GX 2518 HPGe detector was utilized. The gamma spectrometer had a relative efficiency of 25% and allowed for the measurement of induced activity across a wide energy range from 3 keV to 3 MeV/

Prior to measuring the induced activity of minerals, the gamma-ray spectrometer was calibrated using a set of reference gamma-spectrometric sources (cesium-137, cobalt-60, barium-133, americium-241).

Prior to measuring the induced activity of the minerals, the gamma-ray spectrometer was calibrated using a series of reference gamma-spectrometric sources, including cesium-137, cobalt-60, barium-133, and americium-241. The neutron activation analysis revealed the main activated radioisotopes in the minerals with long half-lives, listed in descending order: tantalum-182 ($T_{1/2} = 9.91 \cdot 10^6$ s), europium-152 ($T_{1/2} = 4.27 \cdot 10^8$ s), cesium-134 ($T_{1/2} = 6.53 \cdot 10^7$ s), manganese-54 ($T_{1/2} = 2.70 \cdot 10^7$ s), and scandium-46 ($T_{1/2} = 7.24 \cdot 10^6$ s). Five different screen variants were chosen: option 1 – boron carbide (B4C), option 2 – cadmium, option 3 – tantalum, option 4 – boron carbide and tantalum, option 5 – boron carbide and cadmium.

A study was undertaken to evaluate the influence of various screen materials on the neutron energy distribution within the irradiation device, as shown in Table 8. The "screenless" configuration represented the absence of any screen in the topaz irradiation setup. In this setup, the ratio between the flux of fast neutrons and the flux of thermal neutrons was approximately equal to one. As a result, there was a substantial activation of impurities in the topaz due to the comparable accumulation of fluence from thermal and fast neutrons.

Table 8 presents the findings from the examination of various screens and their influence on the energy distribution of neutrons within the device.

**Table 8 –** Energy distribution of the neutron flux in the irradiation case

| **Option No.** | **< 0.625 eV thermal neutrons** | **0.625 eV – 0.1 MeV suprathermal neutrons** | **> 0.1 MeV fast neutrons** | **Correlation $\Phi_{бн}/\Phi_{тн}$** |
|---|---|---|---|---|
| **Without screens** | 9.16E+13 | 9.72E+13 | 9.04E+13 | 1 |
| **Option number 1** | 1.70E+13 | 7.88E+13 | 8.04E+13 | 4,7 |
| **Option number 2** | 6.67E+13 | 8.90E+13 | 8.64E+13 | 1,3 |
| **Option number 3** | 2.39E+13 | 8.91E+13 | 8.40E+13 | 3,5 |
| **Option number 4** | 1.54E+13 | 7.44E+13 | 7.86E+13 | 5,1 |
| **Option number 5** | 1.54E+13 | 7.62E+13 | 8.08E+13 | 5,2 |

Option 1, 4, and 5 exhibited the highest ratios of fast neutron flux to thermal neutrons, as indicated in Table 8. However, it should be noted that the thermal neutron intensity for option 1 was approximately 10% greater than that of options 4 and 5. Furthermore, option 1 demonstrated a slightly higher proportion of thermal and superthermal neutrons. Notably, the utilization of multilayer screens (options 4 and 5) resulted in the most effective removal of thermal neutrons (reaching up to ~1.5 * $10^{13}$ $cm^{-2}s^{-1}$) and overthermal neutrons (reaching up to ~7.5*$10^{13}$ $cm^{-2}s^{-1}$). Meanwhile, the intensity

of fast neutrons remained consistently high at around ~8 *$10^{13}$ $cm^{-2}s^{-1}$. These conditions minimize impurity activation and facilitate the formation of color centers in topaz.
Upon analyzing the cross section of radiation neutron capture by tantalum and cadmium [28], it can be deduced that the cross-section for tantalum is higher in the resonant part, specifically within the neutron energy range of approximately 1–400 eV. As a result, opting for a tantalum screen is more advantageous. Furthermore, the primary radioisotope activated in topaz was found to be tantalum-182. Hence, employing tantalum as a shield will effectively attenuate neutrons with energies that activate tantalum in topaz.
Table 9 presents the energy release of the materials used in the irradiation device for the five screen variants. The energy release values correspond to the center plane of the core (region I in Figure 8), while the energy release in regions II and III is approximately 10% lower.

**Table 9 -** Heat dissipation of materials of the experimental device

| Variant | Material | Radiative heating, W/g | Density, g/cm$^3$ | Radiative heating, W/cm$^3$ |
|---|---|---|---|---|
| **1** | SAV-1 (pencil case wall) | 2.77 | 2.7 | 7.48 |
| | $B_4C$ (screen inside the pencil case) | 34.47 | 2.52 | 86.86 |
| | Topazes | 2.90 | 3.56 | 10.32 |
| **2** | SAV-1 (pencil case wall) | 2.86 | 2.7 | 7.72 |
| | Tantalum (screen inside the pencil case) | 6.02 | 16.65 | 100.25 |
| | Topazes | 2.96 | 3.56 | 10.54 |
| **3** | SAV-1 (pencil case wall) | 2.65 | 2.7 | 7.16 |
| | Cd (screen inside the pencil case) | 25.99 | 8.65 | 224.8 |
| | Topazes | 2.89 | 3.56 | 10.29 |
| **4** | SAV-1 (pencil case wall) | 2.51 | 2.7 | 6.74 |
| | Tantalum | 5.31 | 16.65 | 88.43 |
| | Boron carbide | 28.95 | 2.52 | 72.95 |
| | Boron carbide | 2.69 | 3.56 | 9.58 |
| **5** | SAV-1 (pencil case wall) | 2.64 | 2.7 | 7.13 |
| | Cadmium | 16.00 | 8.65 | 138.4 |
| | Boron carbide | 21.11 | 2.52 | 53.2 |
| | Topazes | 2.83 | 3.56 | 10.07 |

The utilization of a shield to restrict photon radiation can effectively reduce energy release, as the primary contributor to energy release is the interaction between structural materials and gamma radiation. However, in this particular investigation, shields that limit photon radiation were not taken into account. This decision was made due to the presence of an efficient coolant and the favorable thermal conductivity of the aluminum alloy, which served as the primary material for the capsule.
The figures below illustrate the results of computer simulations depicting the thermal field in the irradiation unit for all screen variations. Each option was assessed under two cooling conditions: forced cooling and natural convection only. In the forced cooling mode, the water velocity at the upper boundary of the region (Figure 15) was set to $V_{in}$ = 0.3 m/s. Conversely, in the mode without forced cooling, the water velocity at the upper boundary of the region (Figure 18) was set to $V_{in}$ = 0.0001 m/s. For both modes, convective heat transfer in accordance with the Navier–Stokes law was applied at the upper and lower boundaries of the water region.

*Option number 1. Radiation shield - $B_4C$ (see Table 2):*

The mode of forced cooling, the velocity of water at the upper boundary of the domain (Figure 15) is equal to $V_{in}$ = 0.3 m / s. Convective heat transfer according to the Navier-Stokes law operates at the same boundary.

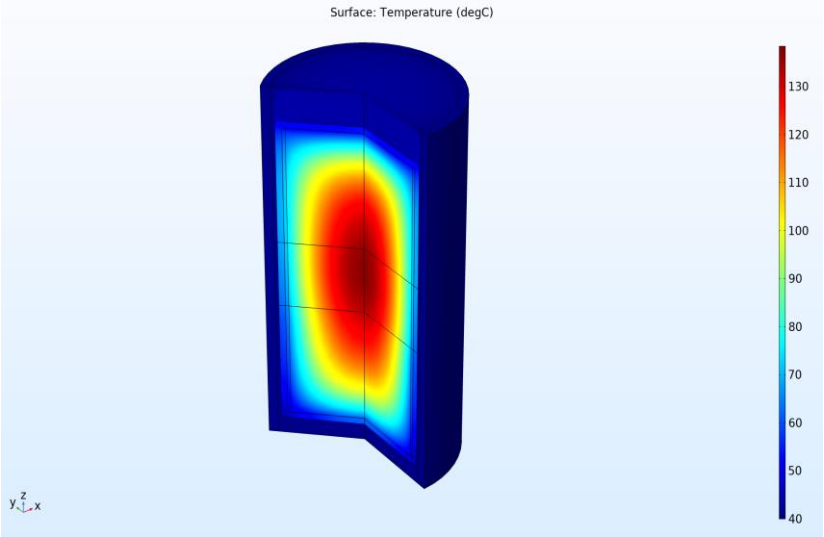


**Fig.14 -** The reconstruction of the stationary temperature field in the modeled region during the forced cooling of the pencil case in three dimensions

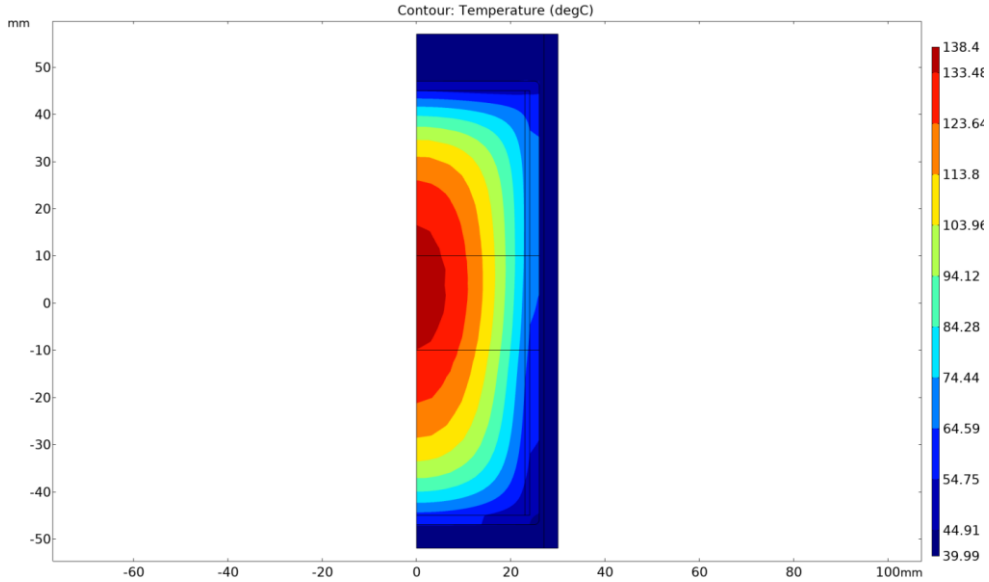


**Fig.15 –** The two-dimensional reconstruction of the stationary temperature field in the modeling area for problem No. 1 with the application of forced cooling to the pencil case

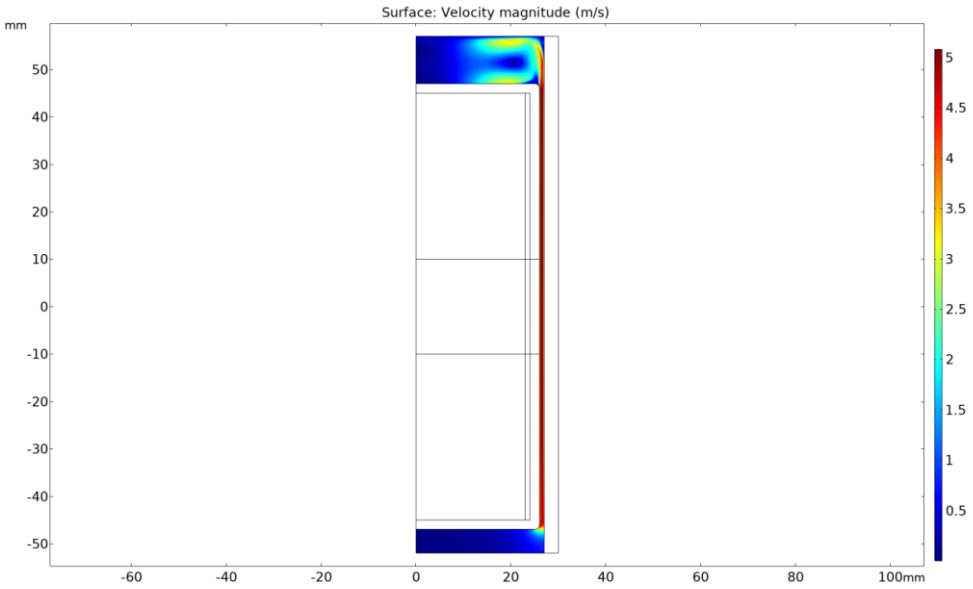


**Fig.16 –** Distribution of the stationary velocity of water movement for task No. 1 during forced cooling of the pencil case

The mode of off cooling, the water velocity at the upper boundary of the domain (Figure 17) is equal to $V_{in}$ = 0.0001 m / s. Convective heat transfer according to the Navier-Stokes law operates at the upper and lower boundaries of water.

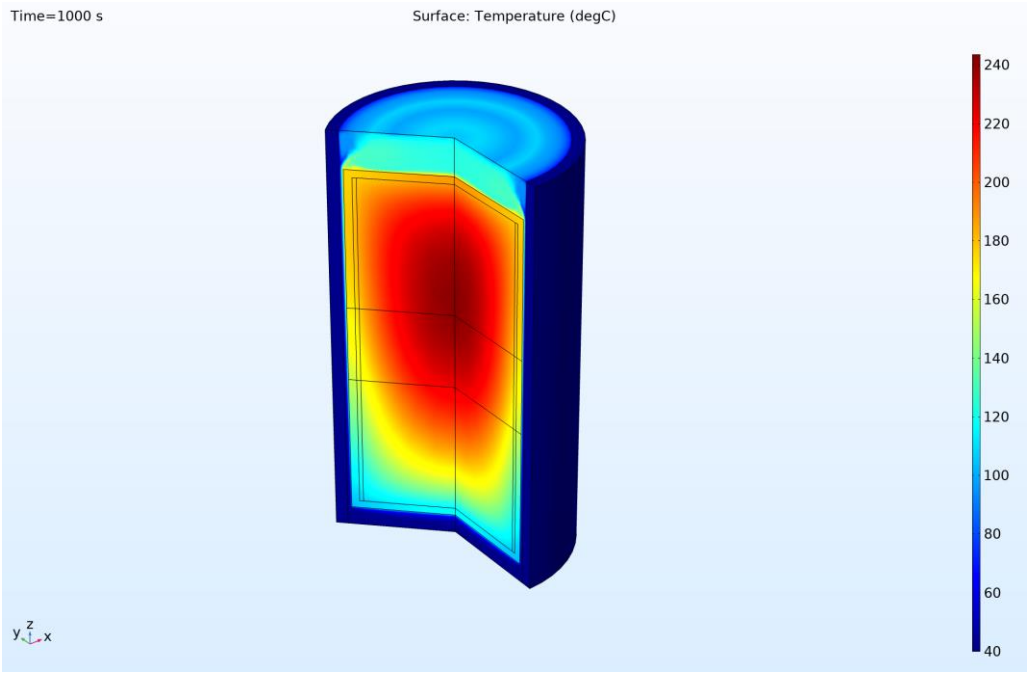


**Fig.17 –** Three-dimensional reconstruction of the stationary temperature field (at time t = 1000 seconds) in the modeling area in the absence of forced cooling of the pencil case

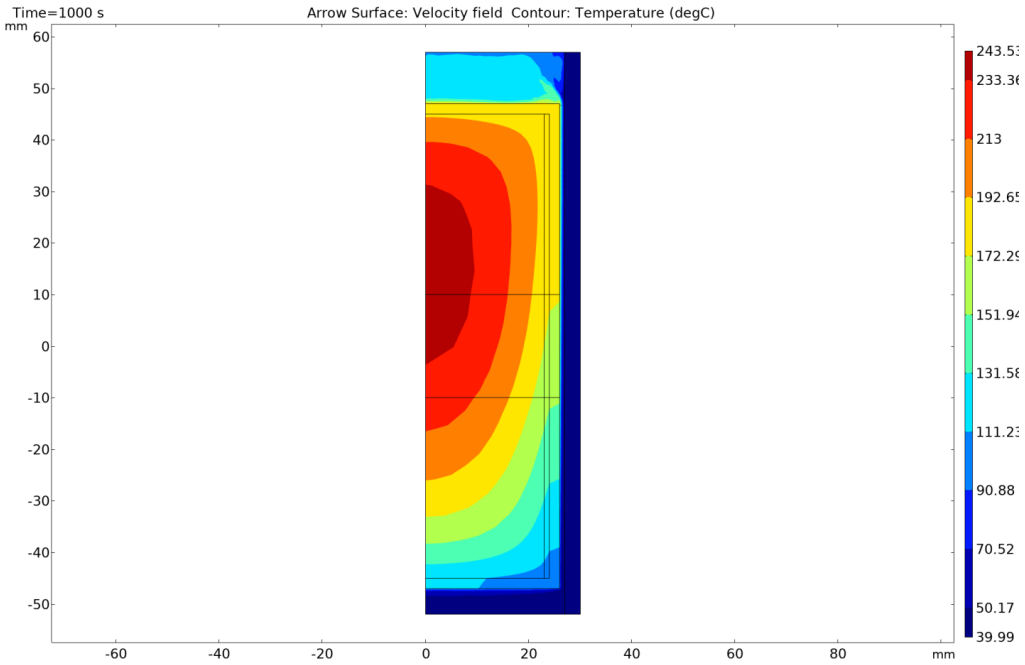


**Fig.18 –** Profile of the stationary temperature field (at time t = 1000 seconds) in the modeling area in the absence of forced cooling of the case (task No. 1)

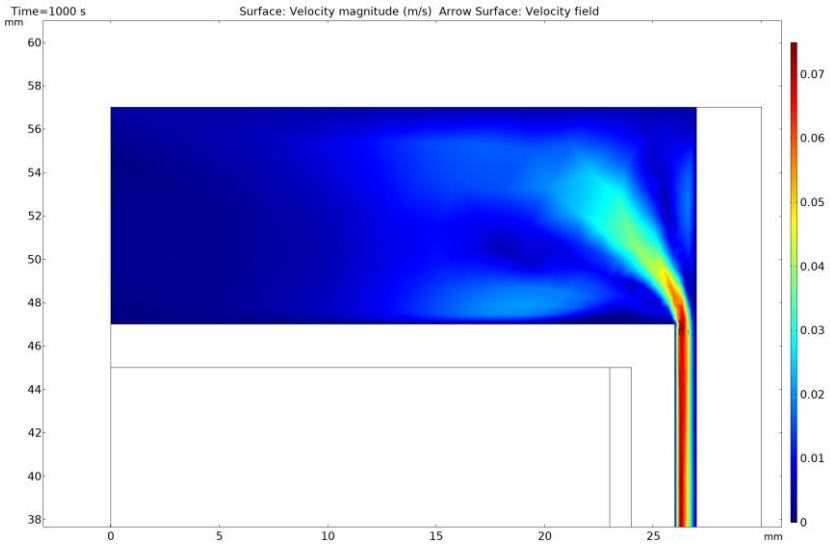


**Fig.19 -** Stationary distribution of water convection velocities (at time t = 1000 seconds) in the modeling area in the absence of forced cooling of the case (task No. 1)

*Option number 2. Radiation shield – Tantalum (see Table 3):*

The mode of forced cooling, the water velocity at the upper boundary of the domain (Figure 21) is equal to $V_{in}$ = 0.3 m / s. Convective heat transfer according to the Navier-Stokes law operates at the upper and lower boundaries. In this scenario, the temperature of the topaz will rise to 130 ° C.

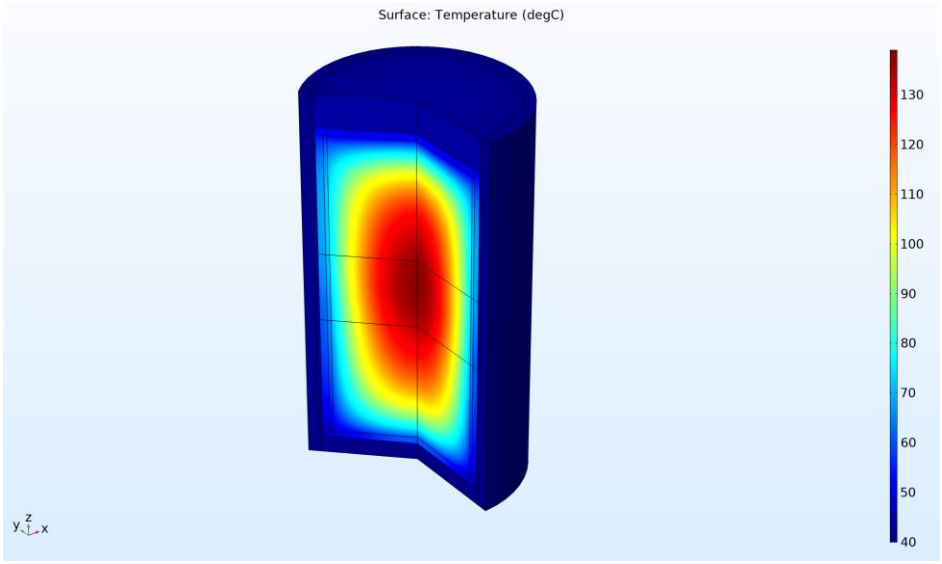


**Fig.20 -** Three-dimensional reconstruction of the stationary temperature field in the modeling area during forced cooling of the pencil case

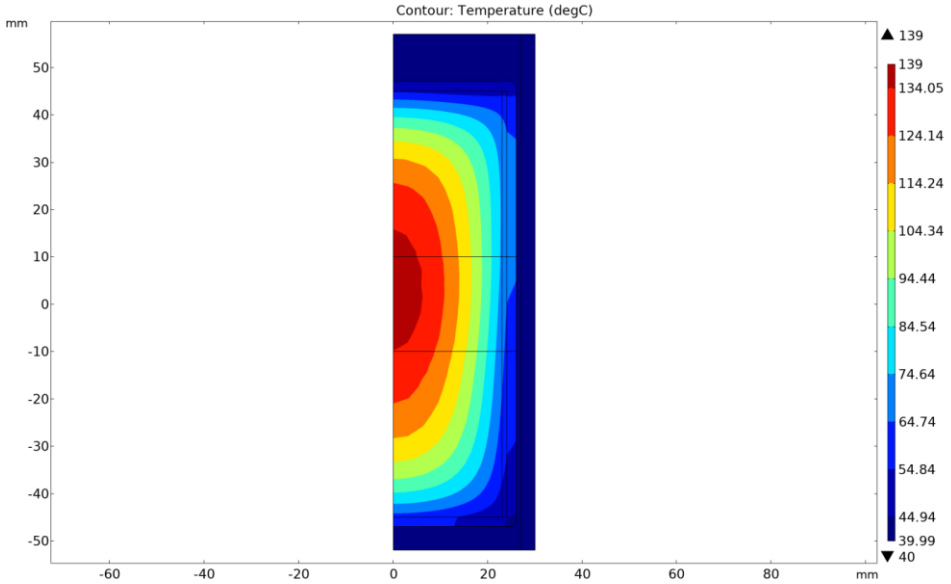


**Fig.21 -** Profile of the distribution of stationary temperature in the modeling area during forced cooling of the pencil case for task No. 2

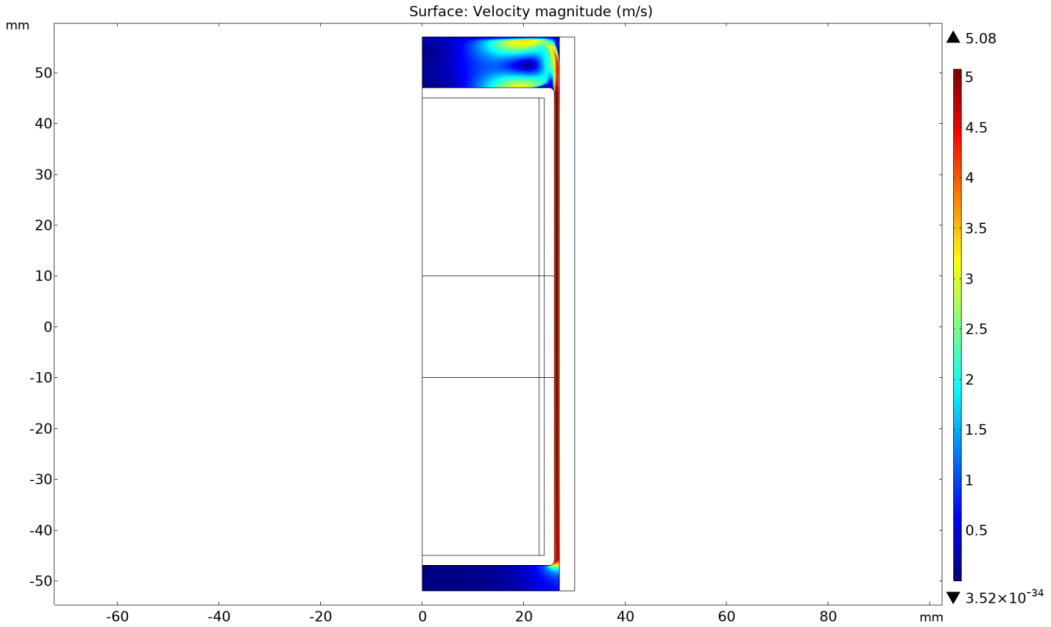


**Fig.22 -** Distribution of the stationary velocity of water movement for task No. 2 during forced cooling of the pencil case

The cooling mode is off, the water velocity at the upper boundary of the domain (Figure 24) is equal to $V_{in}$ = 0.0001 m / s. Convective heat transfer according to the Navier-Stokes law operates at the upper and lower boundaries of water. In this scenario, the temperature of topaz will rise to 240 °C.

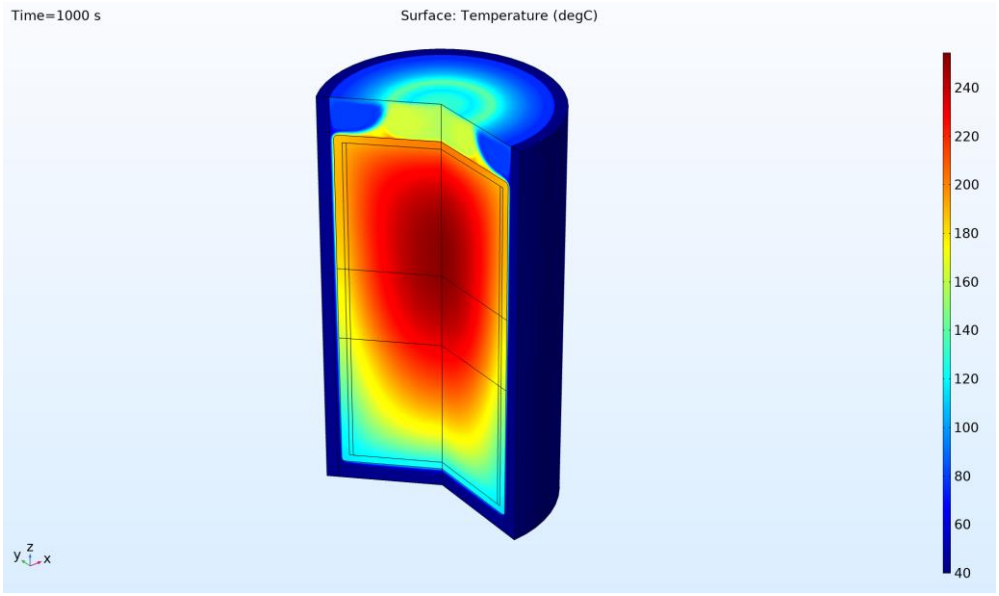


**Fig.23 –** Three-dimensional reconstruction of the stationary temperature field (at time t = 1000 seconds) in the modeling area in the absence of forced cooling of the pencil case

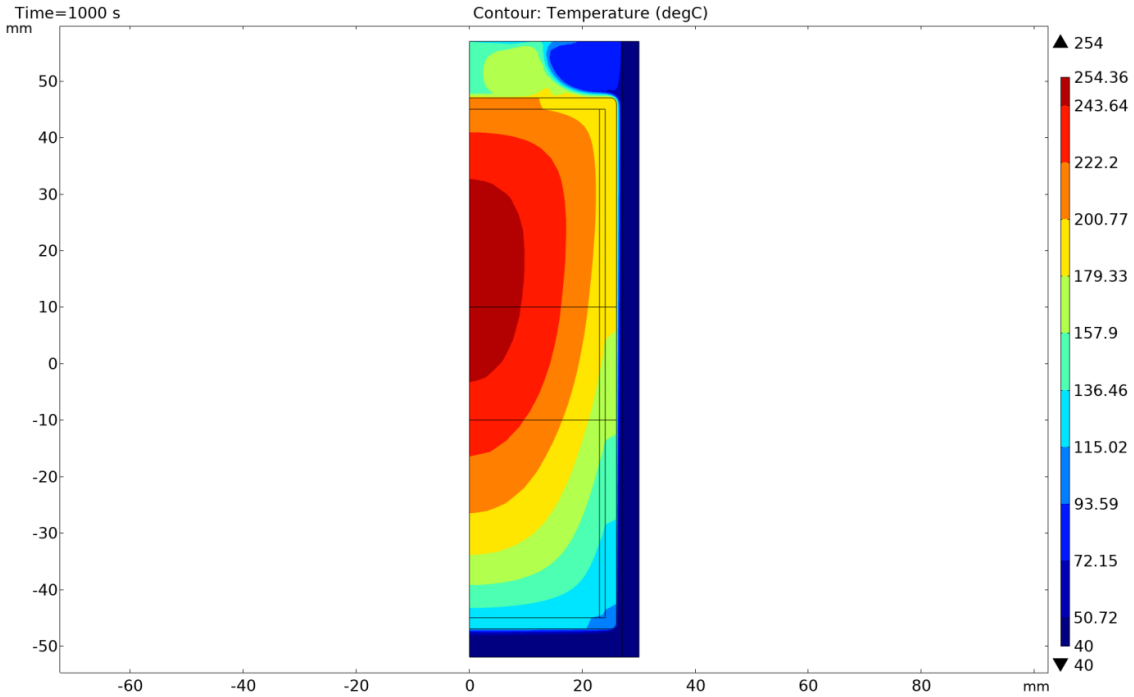


**Fig.24 –** Profile of the stationary temperature field (at time t = 1000 seconds) in the modeling area in the absence of forced cooling of the pencil case (task No. 2)

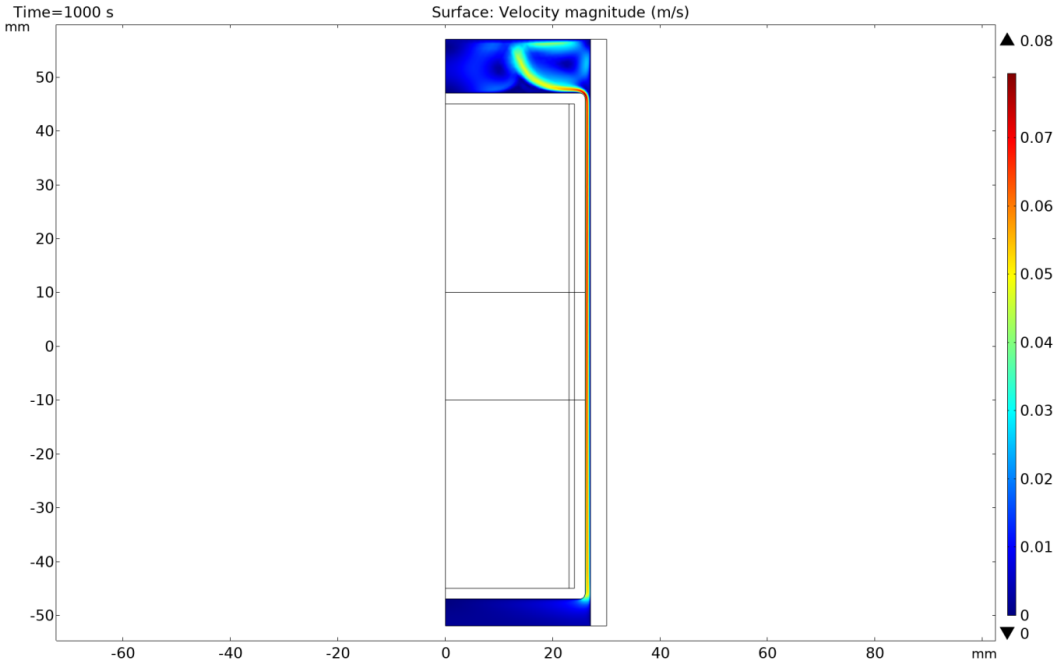


**Fig.25 -** Stationary distribution of the water convection velocity (at time t = 1000 seconds) over the modeling area in the absence of forced cooling of the case (task No. 2)

*Option number 3. Radiation shield – Cadmium:*

Forced cooling mode with water ($V_{in}$ = 0.3 m/s). Convective heat transfer according to the Navier-Stokes law operates at the upper and lower boundaries. In this scenario, the temperature of the topaz will rise to 140 °C.

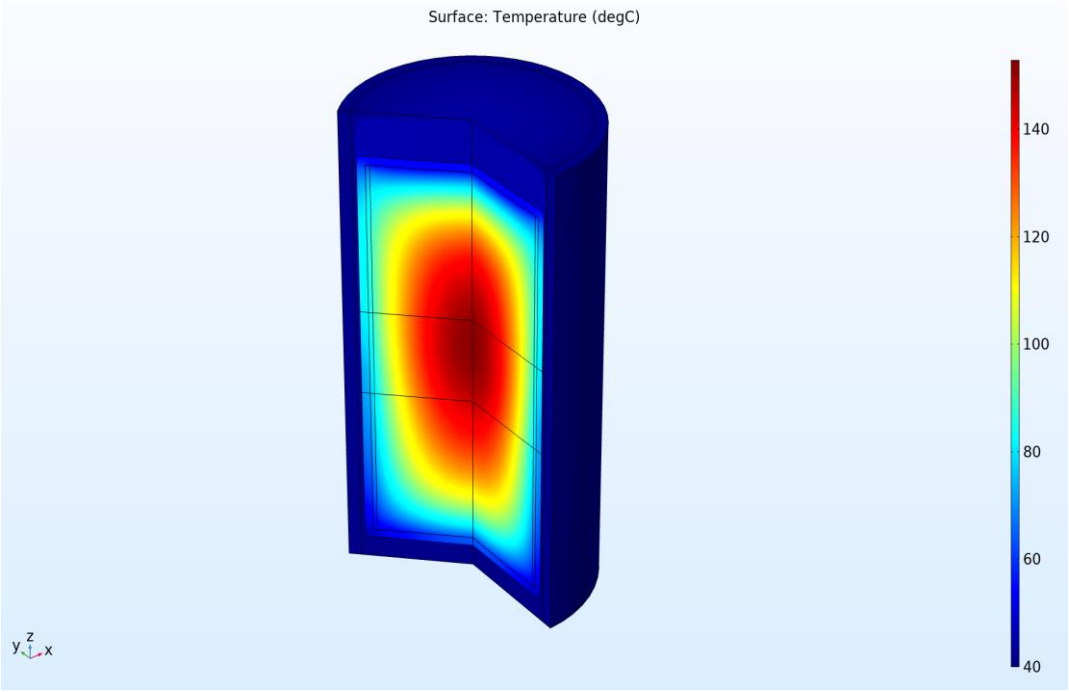


**Fig.26 -** Three-dimensional reconstruction of the stationary temperature field in the modeling area during forced cooling of the pencil case

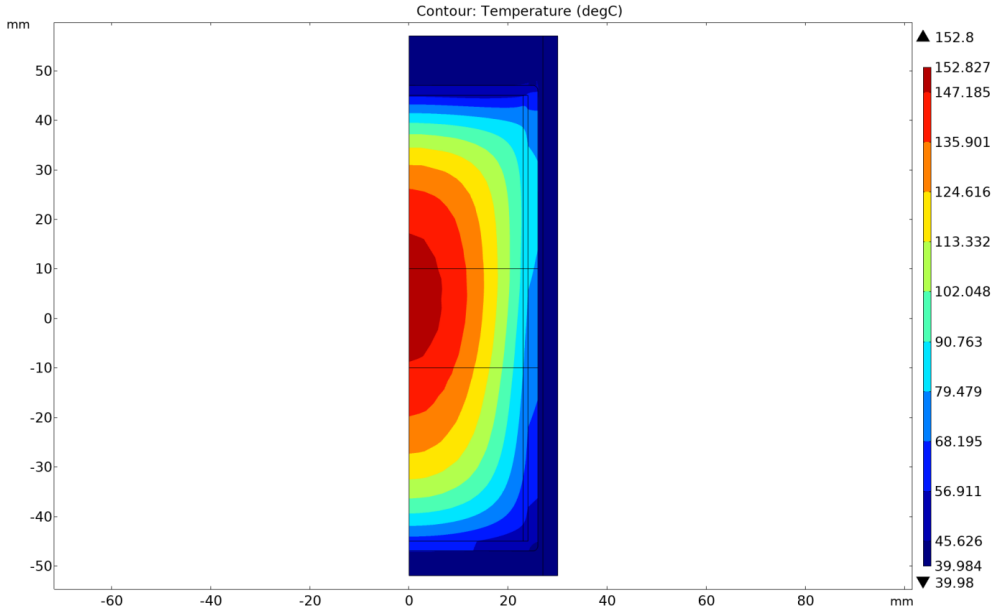


**Fig.27 –** Two-dimensional reconstruction of the stationary temperature field in the modeling area for task No. 3 with forced cooling of the pencil case

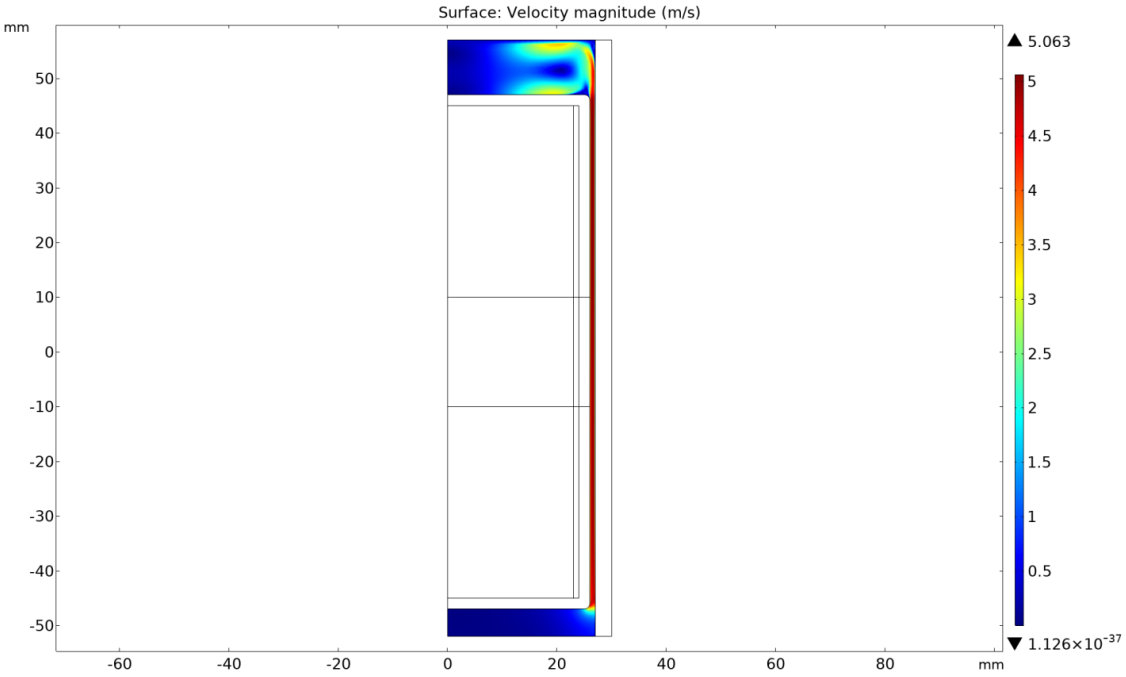


**Fig.28 -** Distribution of the stationary velocity of water movement for task No. 3 during forced cooling of the pencil case

*Mode without water supply.* The velocity of water supply at the upper boundary of the domain (Figure 30) is equal to $V_{in}$ = 0.0001 m/s. Convective heat transfer acts at the upper and lower boundaries of water. In this scenario, the temperature of the topaz will rise to 300 °C.

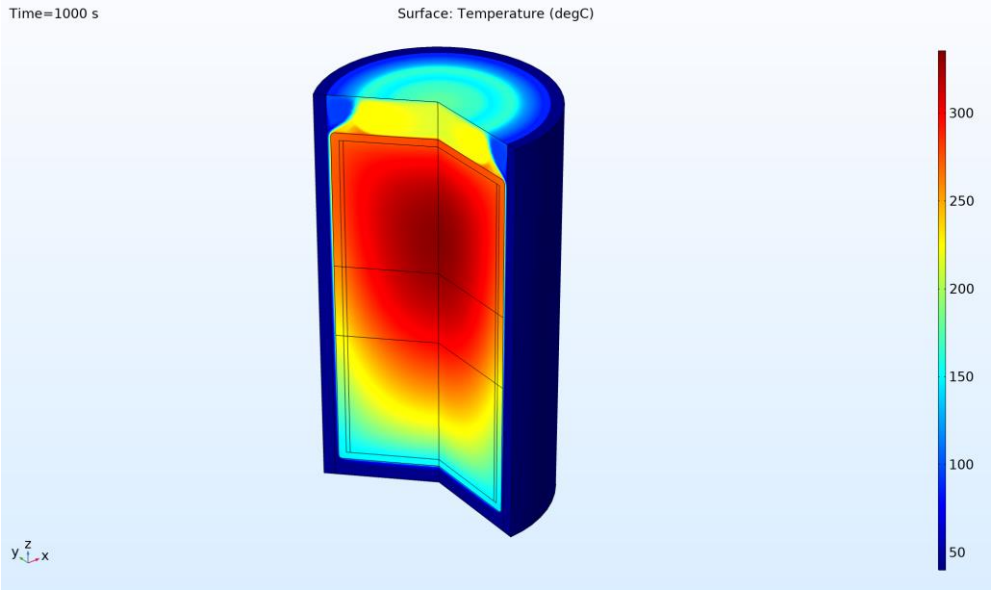


**Fig.29 –** Stationary temperature field (at time t = 1000 seconds) in the modeling area in the absence of forced cooling of the pencil case

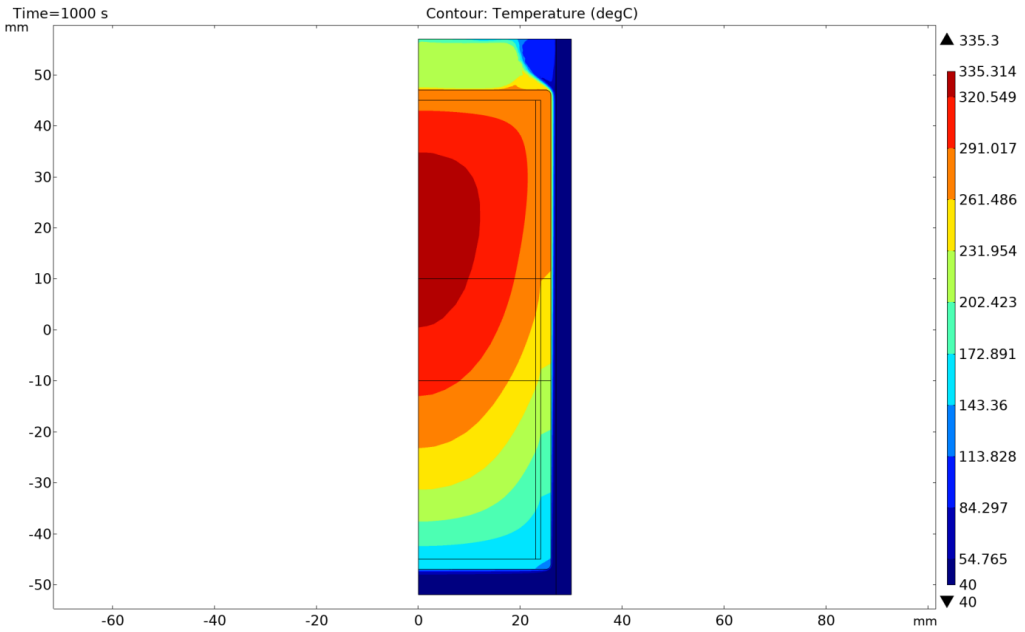


**Fig.30 –** Profile of the stationary temperature field (at time t = 1000 seconds) in the modeling area in the absence of forced cooling of the case (task No. 3)

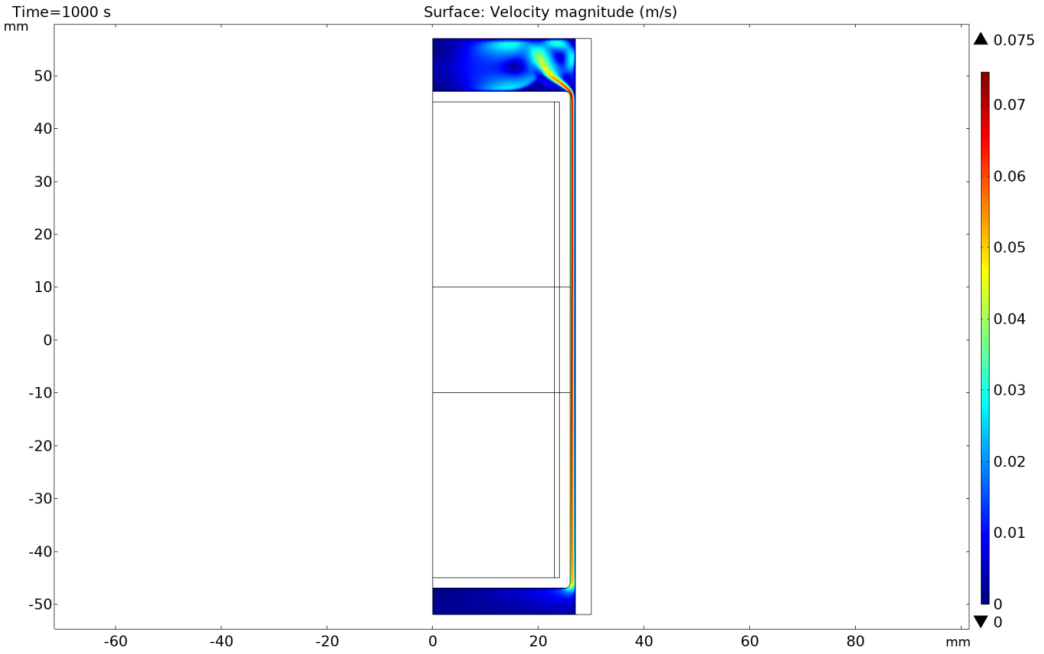


**Fig.31 –** Stationary distribution of water convection velocities (at time t = 1000 s) in the modeling area in the absence of forced cooling of the case (task No. 3)

*Option number 4. Tantalum+Boron Carbide:*

Forced cooling, the water supply rate at the upper limit of the model $V_{in}$ = 0.3 m/s, the temperature of the topaz is up to 130 °C.

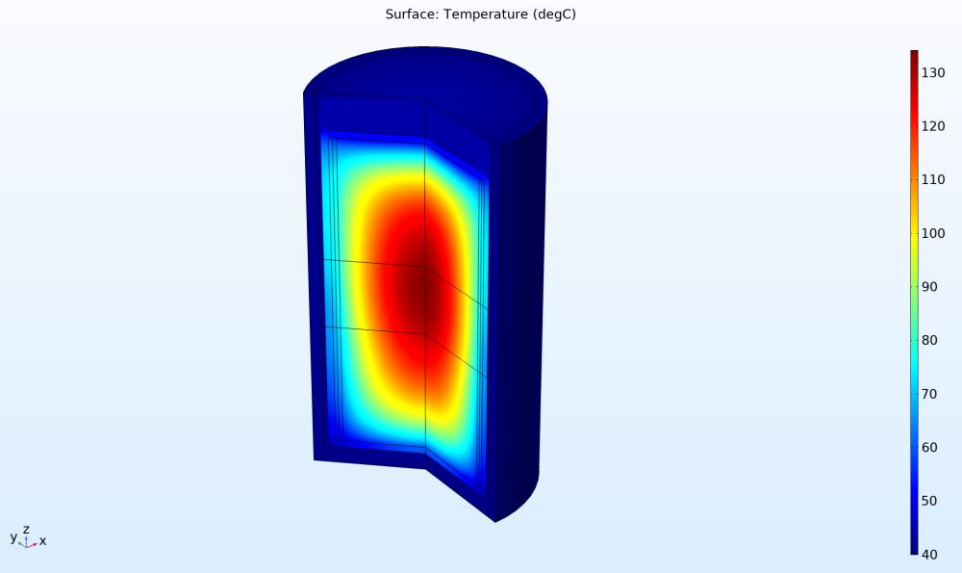


**Fig.32 –** Three-dimensional reconstruction of the stationary temperature field in the modeling area during forced cooling of the pencil case

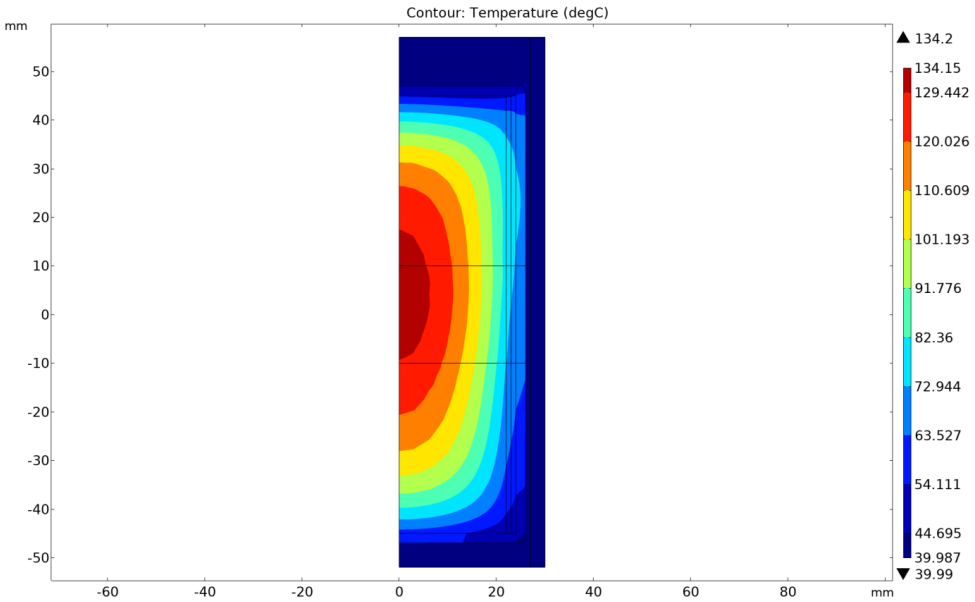


**Fig.33 -** Temperature field profile in the modeling area for task No. 4 during forced cooling of the pencil case

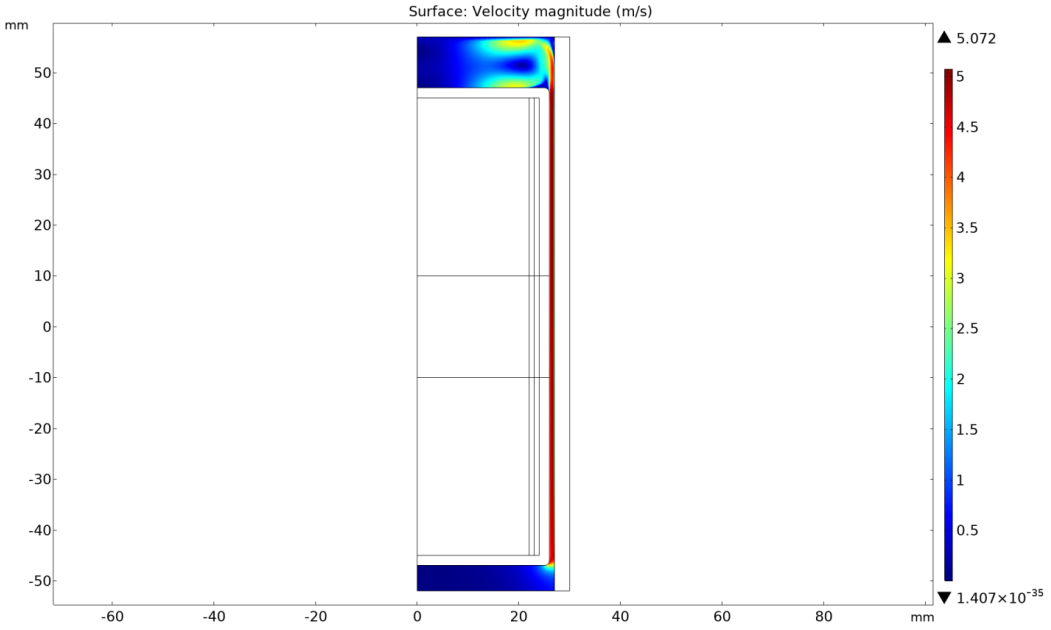


**Fig.34 -** Water velocity in the modeling area for task No. 4 with forced cooling of the pencil case

When the water supply is turned off $V_{in} = 0$, the temperature of the topaz rises to 250 °C.

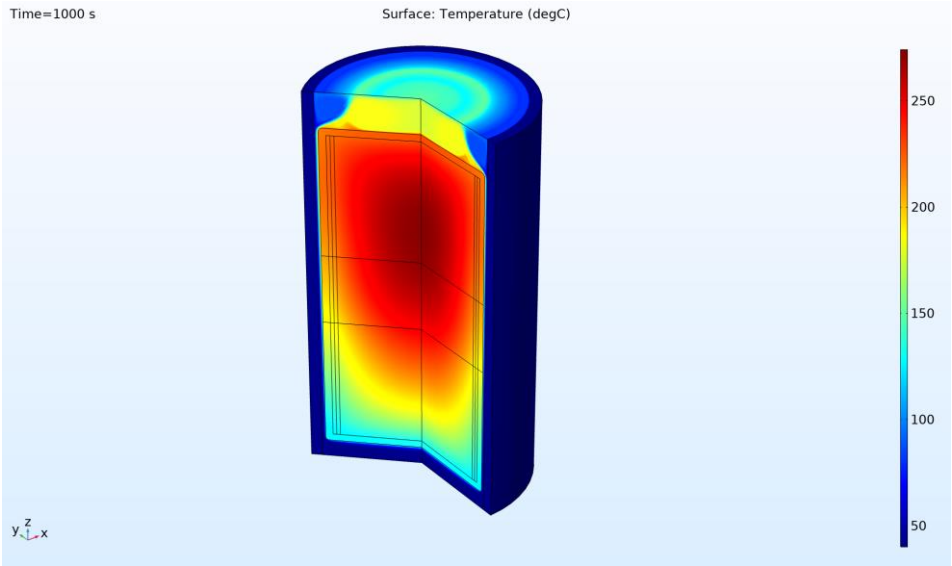


**Fig.35 –** Three-dimensional reconstruction of the stationary temperature field (at time t = 1000 seconds) in the modeling area in the absence of forced cooling of the pencil case

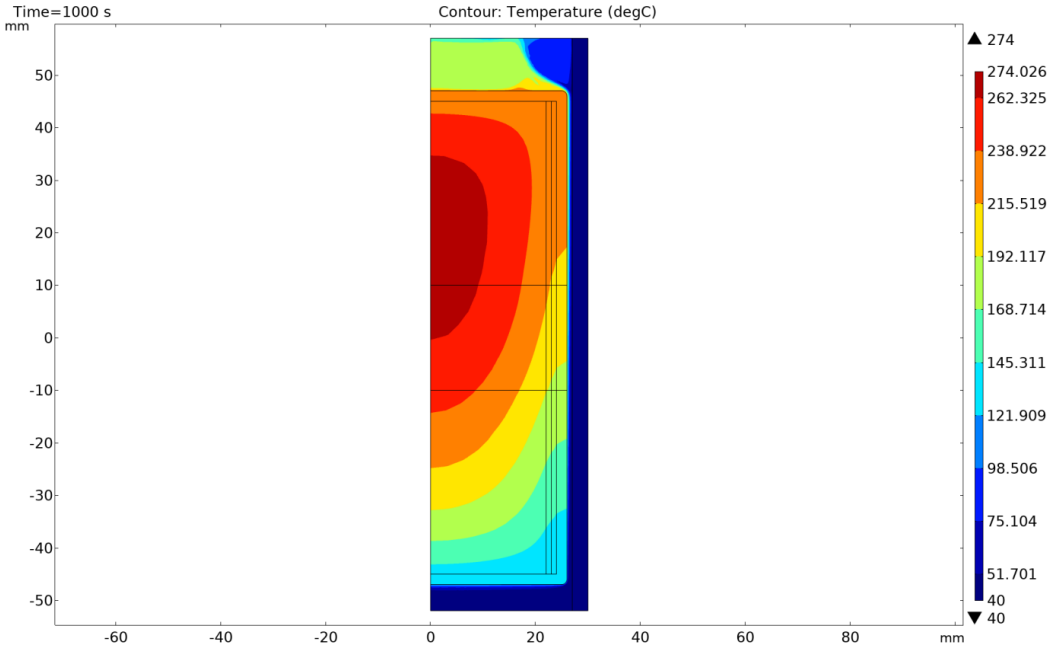


**Fig.36 -** The temperature distribution within the modeling area (at a time of t = 1000 seconds) without the implementation of active cooling for the pencil case (designated as task No. 4)

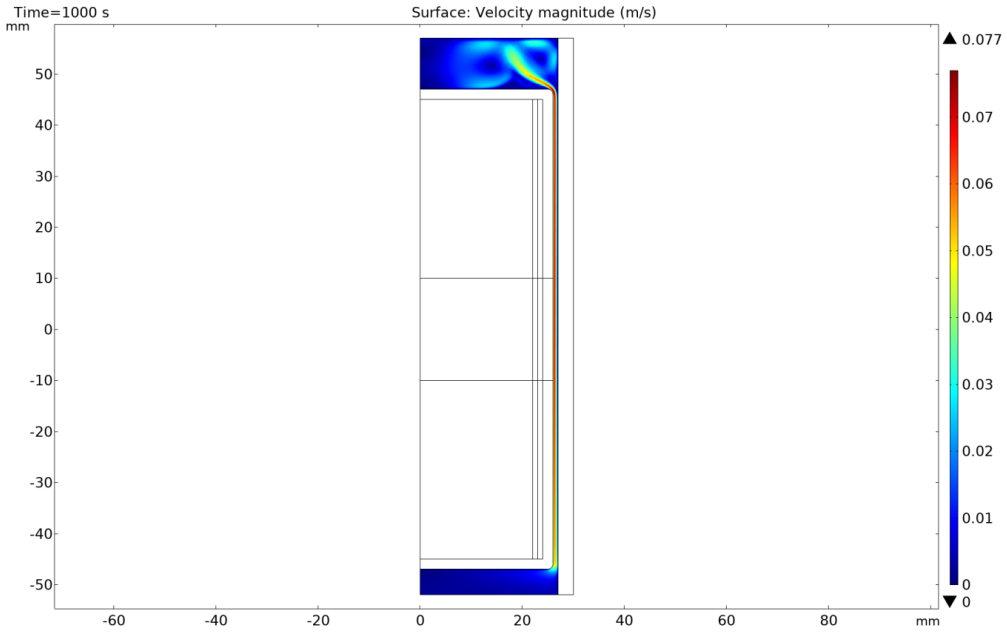


**Fig.37 –** Stationary distribution of the rate of convection of water (at time t = 1000 seconds) in the modeling area in the absence of forced cooling (task No. 4)

*Option number 5. Radiation Shield - Cadmium+Boron Carbide:*

Forced cooling, water flow rate at the upper limit of the model $V_{in}$ = 0.3 m/s.

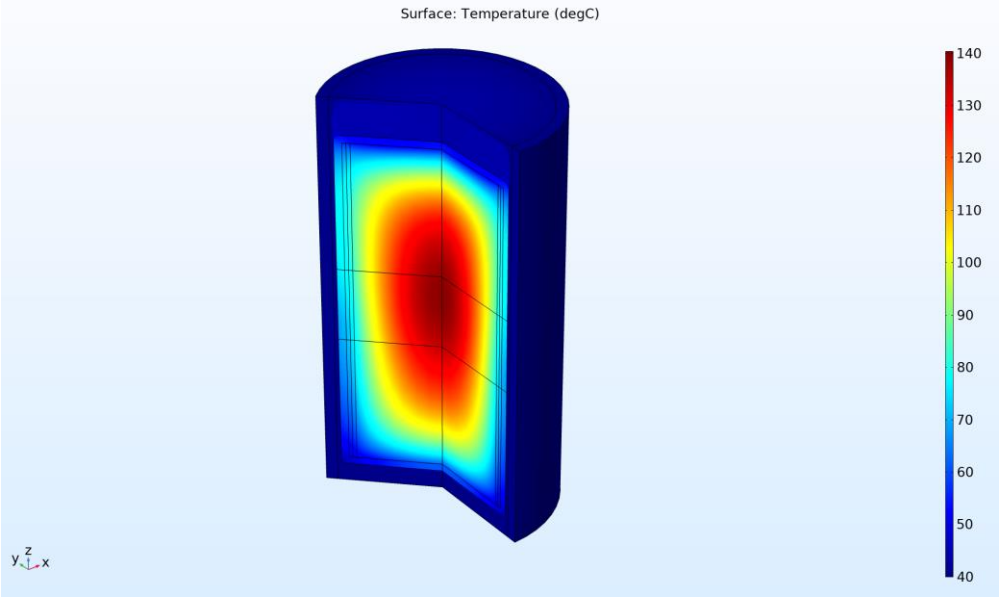


**Fig.38 –** A comprehensive three-dimensional reconstruction of the steady-state temperature distribution within the modeling area while actively cooling the pencil case

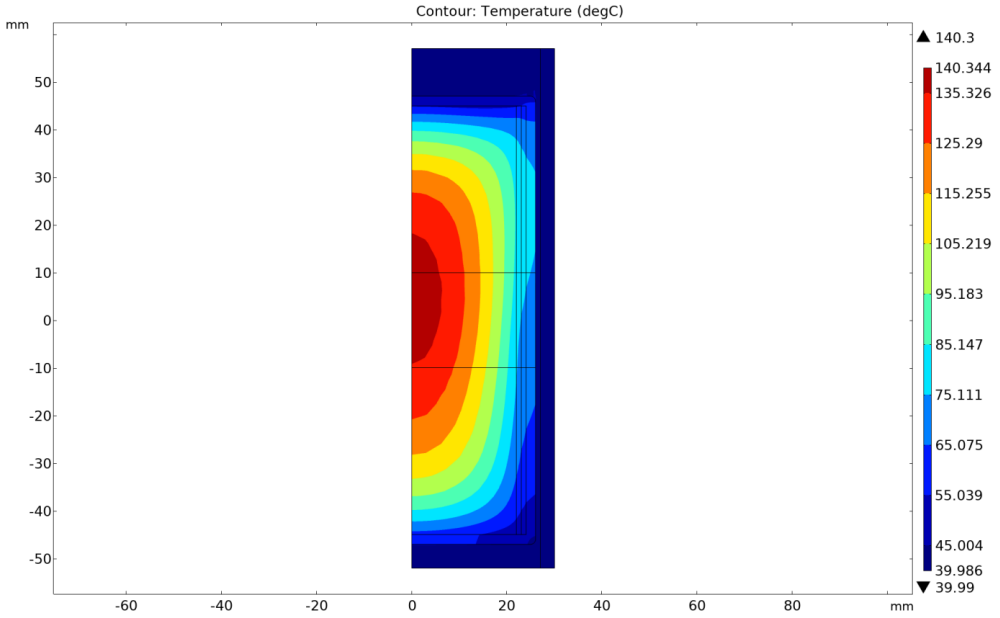


**Fig.39 –** A detailed two-dimensional reconstruction of the steady-state temperature distribution within the modeling area for scenario number 5, involving the active cooling of the pencil case

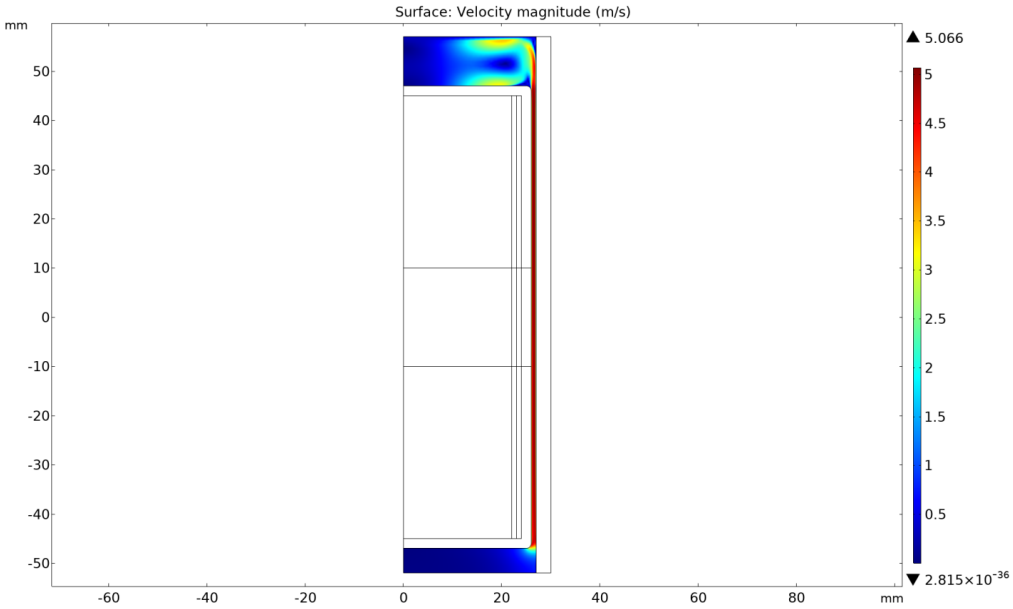


**Fig.40 –** Stationary water velocity for task No. 5 with forced cooling of the pencil case

When the water supply is turned off $V_{in}$ = 0, the maximum temperature of the topaz rises to 300 ° C.

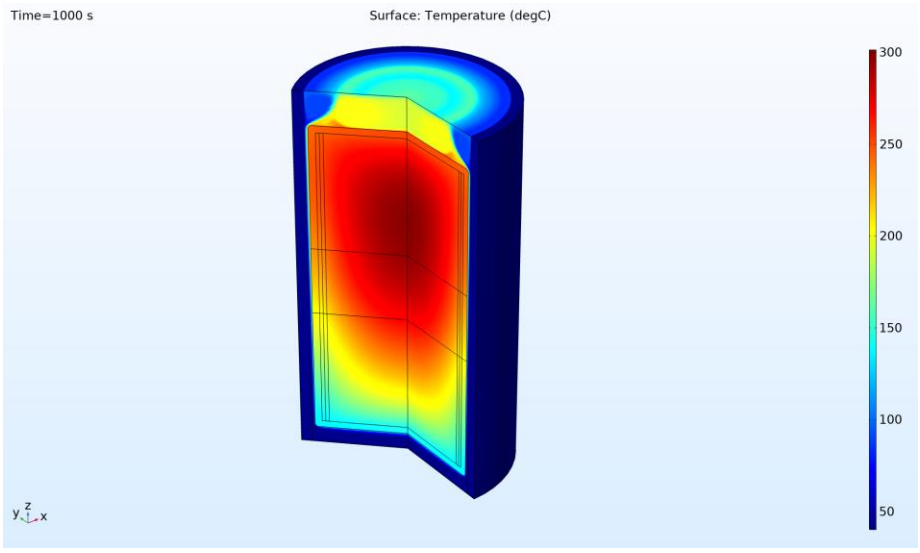


**Fig.41 –** A comprehensive three-dimensional visualization of the temperature distribution within the modeling area at a specific time point (t = 1000 seconds), depicting the scenario without any imposed forced cooling of the pencil case

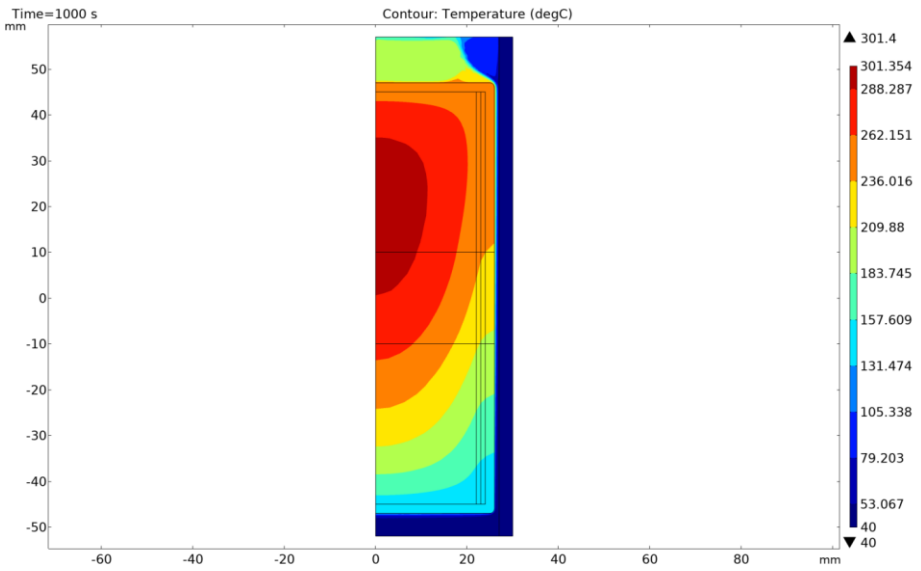


**Fig.42 –** Profile of the stationary temperature field (at time t = 1000 seconds) in the modeling area in the absence of forced cooling of the pencil case (task No. 5)

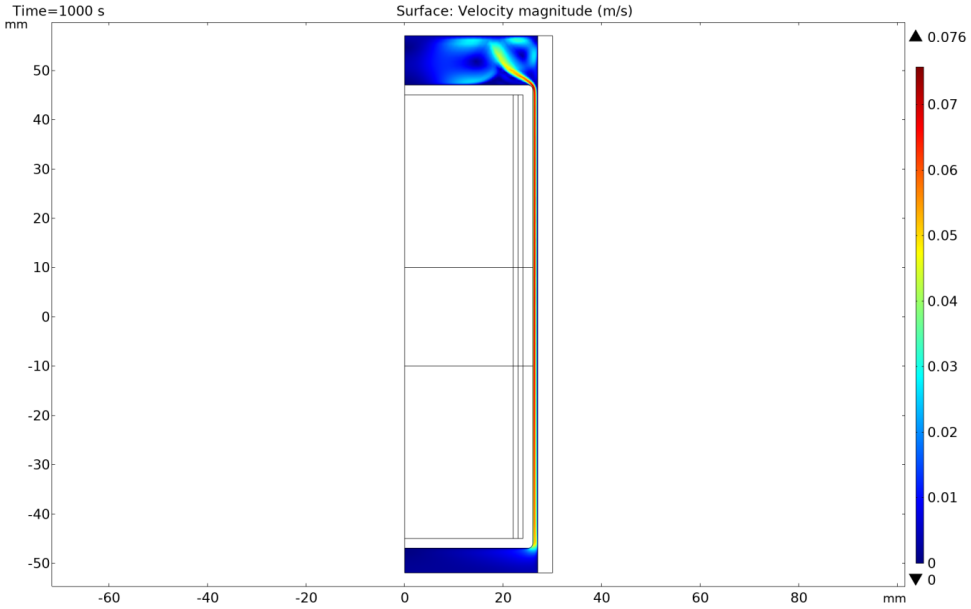


**Fig.43 -** Stationary distribution of the rate of convection of water (at time t = 1000 seconds) in the modeling area in the absence of forced cooling (task No. 5)

Table 10 provides the highest temperatures of the screen's outer wall and topaz for each considered variant. The analysis reveals that option 4, chosen based on neutron analysis, proves to be more favorable. During regular operation, the temperature of topaz remains lower and does not exceed 134 °C. In the event of a coolant circulation failure, leading to an emergency mode, the maximum topaz temperature rises to 274 °C, which is 26 °C lower compared to option 5.

**Table 10 –** Highest temperatures in the irradiation device

| Conditions | Cooling mode | The highest temperature of the outer surface of the screen wall, °C | Highest temperature of topaz, °C |
|---|---|---|---|
| 1 | Without refrigeration | 69 | 138 |
| | With refrigeration | 187 | 242 |
| 2 | Without refrigeration | 69 | 139 |
| | With refrigeration | 193 | 254 |
| 3 | Without refrigeration | 83 | 153 |
| | With refrigeration | 276 | 335 |
| 4 | Without refrigeration | 75 | 134 |
| | With refrigeration | 238 | 274 |
| 5 | Without refrigeration | 79 | 140 |
| | With refrigeration | 252 | 300 |

Nevertheless, the findings presented above were derived under a cautious methodology that neglected the water circulation between the minerals. As a result, a supplementary computation was conducted to explore the scenario more realistically, focusing solely on option 4. In this revised calculation, the water velocity between the topazes was adjusted to account for the deceleration caused by the reduction in flow area, resulting in a velocity of 0.0225 m/s.

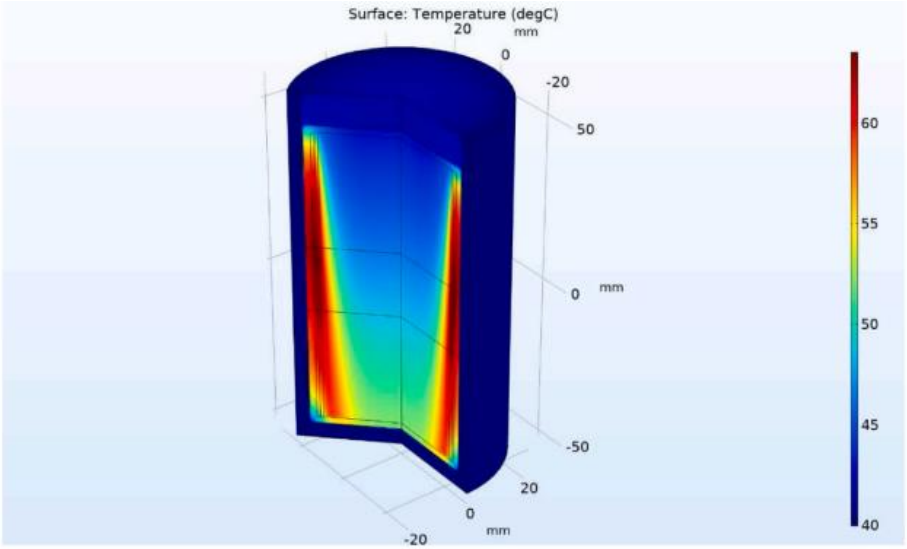


**Fig.44 –** A comprehensive three-dimensional reconstruction was conducted to visualize the stationary temperature distribution within the modeling zone of the irradiation installation, specifically for option 4. This detailed reconstruction provides valuable insights into the thermal characteristics and behavior of the system under consideration

The findings depicted in Figure 44 unmistakably demonstrate a significant alteration in the temperature field profile, with the maximum temperature of topaz being well below 65 °C. The modeling results emphasize the crucial role of mineral circulation during irradiation, as it effectively reduces the mineral temperature by nearly half, highlighting its significance in optimizing the thermal behavior of the system.

Analyzing the results of thermophysical calculations and analyzing various designs of the experimental device, we can draw the following conclusions:

1) With forced water cooling of the pencil case with water with a temperature of 40 ° C with an input speed of 0.3 m / s, the temperature of the case body will be from 50 ° C to 70 ° C and will not exceed 80 ° C for all considered options (tasks 1-5);
2) With this forced cooling, the temperature of the topaz samples will be in the range from 50°C (in the bottom and top cover areas) to 145°C (in the upward offset center of the case) and will not exceed 155°C;
3) When the water supply is cut off (in convection cooling mode), the surface temperature of the pencil case will reach 100 ° C within 20-40 seconds from the moment the flow is turned off and the water on the top cover will begin to boil, further reducing the cooling of the case. After 300-500 seconds, the pencil case will reach equilibrium temperatures, depending on the type of radiation shield, with the distribution as shown in Figures 11,17,23,29 and 35. The maximum design temperatures will be in the central area of the sample location. Values of maximum temperatures depending on the task: No. 1 - 243.5 °C; №2 - 254.3°C; №3 - 335.3°C; №4 - 274°C; №5 - 301.4°C.
4) Task No. 3 (single-layer cadmium shield) has a record heat generation and the samples in it will heat up above 150 °C even with forced water cooling at a speed of 0.3 m/s.

## CONCLUSIONS

Throughout the simulation, the irradiation facility for neutron irradiation of topaz in the WWR-K reactor was examined using five different screen variations. After conducting neutron analysis, two sandwich screen options were chosen: boron and tantalum carbide (option 4) and boron and cadmium carbide (option 5). When utilizing a screen composed of boron carbide and tantalum, minimal activation of Ta-182, a long-lived impurity affecting the cooling duration of topaz, was observed. Thermophysical analysis, employing a cautious approach, indicated that among variants 4 and 5, variant 4 exhibited the lowest temperatures in both forced and natural convection modes. These temperatures were recorded as 134 °C and 274 °C, respectively. Additionally, the temperature of the casing was measured at 75 °C with forced cooling and 238 °C without cooling.

Hence, incorporating the multilayer screen (option 4) into the irradiator design effectively decreases the induced activity of topaz caused by the activation of impurities through thermal and superthermal neutrons. Furthermore, it facilitates the creation of favorable conditions for efficient radiation coloring, specifically the formation of color centers within the crystal lattice. With the consideration of water circulation between topazes, their temperature remains below 65 °C, ensuring compliance with the required temperature regime. This temperature control significantly impacts the optical properties of topaz and, ultimately, enhances their value as gemstones.

## List of References


1. Mironova-Ulmane N., Skvortsova V., Popov A. I., 2016. Optical absorption and luminescence studies of fast neutron-irradiated complex oxides for jewellery applications. Low temperature physics. 42, 584-587. http://dx.doi.org/10.1063/1.4959017
2. A.M. Akhanov, M.T. Aitkulov, D.S. Sairanbayev, Sh.Kh Gizatulin, N.K. Romanova, A.A. Shaimerdenov, Y.V. Chikhray, Zh Ualzhanov, T.K. Zholdybayev, 2022. Irradiation capsule design for neutron coloration of topaz in a WWR-K reactor. Applied Radiation and Isotopes 190. 110472.
3. Krambrock K., Ribeiro L. G. M., Pinheiro M. V. B., Leal A. S., Menezes M. Â. de B. C., Spaeth J.-M., 2007. Color centers in topaz: comparison between neutron and gamma irradiation. Phys Chem Minerals. 34, 437–444. https://doi.org/10.1007/s00269-007-0160-z
4. Mohamed Nader M.A., Gaheen M.A., 2016. Design of fast neutron channels for topaz irradiation. Nuclear Engineering and Design. 310, 429-437. https://doi.org/10.1016/j.nucengdes.2016.11.001
5. Leal A.S., Krambrock K., Ribeiro L.G.M., Menezes M.Aˆ .B.C., Vermaercke P., Sneyers L., 2007. Study of neutron irradiation-induced colors in Brazilian topaz. Nuclear Instruments and Methods in Physics Research A. 580, 423–426. https://doi.org/doi:10.1016/j.nima.2007.05.069
6. Baitelesov S.A., Ibragimova E.M., Kungurov F.R., Salikhbaev U.S., 2011. Effect of the VVR-SM neutron spectrum on the radioactivity and color of natural topazes. Atomic Energy. 109, 355-361.
7. Mi, X. et al., 2019. Design of in-pile topaz color-alteration device. High Power Laser and Particle Beams. 31.
8. International Atomic Energy Agency (IAEA), 2001. The Applications of Research Reactors IAEA-TECDOC-1234. IAEA.
9. Nassau K., 1985. Altering the Color of Topaz. Gems Gemol. 21, 26.
10. J. Zhang et al., 2011. The Radioactive Decay Pattern of Blue Topaz Treated by Neutron Irradiation. Gems Gemol. 47, 302.
11. Safwat Salama Mohamed Soubih Salama, 2011. Study on Properties of Some Treated Gemstones. Thesis. Benha University. 171 p.
12. Godovikov A.A., Varlachev V.A., Solodovnikov E.S., Shcherbakov A.A., Device for irradiation of minerals, Patent of the Russian Federation RU2406170C2.
13. Svyatkin M.N., Izhutov A.L., Romanovsky S.V., Svistunov V.A., Chernov M.F., Isaev Yu.N. Method for irradiating minerals and a device for its implementation, Patent of the Russian Federation RU2341596C2.
14. Merezhko M.S., Merezhko D.A., Rofman O.V., Maksimkin O.P., Short M.P., 2022. Macro-Scale strain localization in highly irradiated stainless steel investigated using digital image correlation. Acta Materialia. 231, 117858.
15. Yarovchuk A.V., Dikov A.S., Tsay K.V., 2022. Peculiarities of stress corrosion fracture of sensitized and neutron irradiated chromium-nickel austenitic steel. Journal of Physics: Conference Series. 2155, 012011.
16. Akaev S.O., Dikov A.S., Dikova L.A., Chernov I.I., Staltsov M.S., 2020. The effect of neutron irradiation in a helium atmosphere on the mechanical properties of 18Cr10NiTi austenitic steel. IOP Conference Series: Materials Science and Engineering. 1005, 012007.
17. Merezhko D.A., Gussev M.N., Merezhko M.S., Rosseel T.M., Garner F.A., 2022. Morphology and elemental composition of a new iron-rich ferrite phase in highly irradiated austenitic steel. Scripta Materialia, 215, 114690.
18. Sairanbayev D., Koltochnik S., Shaimerdenov A., Chakrova Y., Gurin A., Kenzhin Y., 2021. Analysis of lutetium-177 production at the WWR-K research reactor. Applied radiation and isotopes. 169, 109561. https://doi.org/10.1016/j.apradiso.2020.109561

19. Kulsartov T., Gabdullin M., Chikhray Ye., Zaurbekova Zh., Kizane G., Kenzhin Ye., Tolenova A., Nesterov E., Shaimerdenov A., 2021. Experiments on tritium generation and yield from lithium ceramics during neutron irradiation. International Journal of Hydrogen Energy. 46, 9186-9192. https://doi.org/10.1016/j.ijhydene.2020.12.224
20. Kashaykin P.F., Tomashuk A.L., Vasiliev S.A., Ignatyev A.D., Shaimerdenov A.A., Ponkratov Yu.V., Kulsartov T.V., Kenzhin Y.A., Gizatulin Sh. Kh., Zholdybayev T.K., Chikhray Y.V., Semjonov S.L., 2021. Radiation resistance of single-mode optical fibres with view to in-reactor applications. Nuclear Materials and Energy. 27, 100981. https://doi.org/10.1016/j.nme.2021.100981
21. Kulsartov T., Kenzhina I., Chikhray Ye., Zaurbekova Zh., Kenzhin Ye., Gizatulin Sh., Dyussambayev D., Aitkulov M., 2021. Determination of the activation energy of tritium diffusion in ceramic breeders by reactor power variation. Fusion Engineering and Design. 172, 112783. https://doi.org/10.1016/j.fusengdes.2021.112783
22. Kulsartov T., Shaimerdenov A., Zaurbekova Zh., Kenzhina I., Chikhray Y., Kizane G., Blynskiy P., Akhanov A., Ponkratov Yu., 2021. Features of the in-situ experiments on studying of tritium release from lithium ceramic Li2TiO3 using vacuum extraction method. Fusion Engineering and Design. 172, 112783. https://doi.org/10.1016/j.fusengdes.2021.112703
23. Shaimerdenov A. A., Nakipov D. A., Arinkin F. M., Gizatulin Sh. Kh., Chakrov P. V., Kenzhin Ye. A., 2018. The 50th Anniversary of the WWR-K Research Reactor. Physics of Atomic Nuclei. 81, 1408–1411. https://doi.org/10.1134/S1063778818100162
24. Shaimerdenov A., Gizatulin S., Dyussambayev D., Askerbekov S., Kenzhina I., 2020. The WWR-K reactor experimental base for studies of the tritium release from materials under irradiation, Fusion Science and Technology. 76, 304-313. https://doi.org/10.1080/15361055.2020.1711852
25. Goorley J.T., et al., 2013. Initial MCNP6 Release Overview - MCNP6 version 1.0, LA-UR-13-22934.
26. Brown D. A., Chadwick M. B., Capote R., Kahler A. C., Trkov A., Herman M.W. end et. al., 2011. ENDF/B-VII.1 Nuclear Data for Science and Technology: Cross Sections, Covariances, Fission Product Yields and Decay Data. Nuclear Data Sheets. 112, 2887-2996.
27. COMSOL Multiphysics, 2022. https://www.comsol.com/comsol-multiphysics (accessed 25 April 2022).
28. Hoover D.B., 1983. The gem diamond master and the thermal properties of gems. Gems and gemology. 77-86.
29. Nuclear Data Center of KAERI, 2022. http://atom.kaeri.re.kr/ (accessed 21 April 2022).